

**DESIGN AND SIMULATION OF THE
MOTOR-GEAR-ALTERNATOR MODEL TO AMPLIFY
THE USABILITY OF THE SOLAR ENERGY FOR
COMMERCIAL AND DOMESTIC USE**

BY

KOECH WESLEY CHERUIYOT

**A THESIS SUBMITTED IN PARTIAL FULFILMENT OF THE
REQUIREMENTS FOR THE AWARD OF THE DEGREE OF
DOCTOR OF PHILOSOPHY IN APPLIED MATHEMATICS
IN THE SCHOOL OF BIOLOGICAL AND
PHYSICAL SCIENCES,
MOI UNIVERSITY**

©2018

Declaration

Declaration by the Candidate

I the undersigned declare that this thesis is my original work and has not been presented for academic purposes in this University or any other Institution for academic purposes whatsoever. No part of this thesis may be reproduced without written permission from the author and / or Moi university.

Koech Wesley Cheruiyot Date:.....
 PHD/AM/02/14

Declaration by the Supervisors

This thesis has been submitted for examination with our approval as University Supervisors.

Prof. Samwel Rotich Date:.....
 Department of Mathematics and Physics,
 Moi University,
 Eldoret, Kenya.

Dr. Titus Rotich Date:.....
 Department of Mathematics and Physics,
 Moi University,
 Eldoret, Kenya.

Dr. Fredrick Oluoch Nyamwala Date:.....
 Department of Mathematics and Physics,
 Moi University,
 Eldoret, Kenya.

Dedication

I humbly dedicate this work to my mother and father, Eunice Bii and Peter Bii, who first taught me the value of education and critical thinking.

Abstract

The solar energy technology seems a long term reliable and sustainable energy model. Besides, the solar cell and solar power harvesting technology have advanced to the impressive levels. However, solar energy technology is lacking in terms of efficiency and usability. Solar power generating systems can be organized into mini-grids to serve areas not covered by the mains supply. The issue of the depletion of oil reserves in the world, the demand for electricity, frequent power outage and the problem of air pollution produced by motor vehicles emissions which have led to global warming motivate many researchers to seek alternative energy sources. In this study, a mathematical model to represent the MGA dynamics was designed. Detailed mathematical derivations from first principles have been presented and then represented the derived equations within Simulink. The parameters identification was investigated by applying different methods in MGA models. The Nonlinear Least-Square and Pattern-Search strategies were the best methods among the methods studied because of the performance and the accuracy and could be automated in MATLAB. Moreover, the effect of each of the PID parameters on the closed-loop dynamics were discussed and demonstrated how to use a PID controller to improve the system performance. Finally, the stability of the MGA Model was studied using Routh-Hurwitz, Nyquist and Bode plots. It was found that the Bode plot is the best tool for determining the range of the gear ratio while the Nyquist plot and Routh Hurwitz methods are the best to obtain the relative stability of the closed and open system respectively. Simulation showed that the system is stable for $1 \leq G_r \leq 7$ and the excess voltage is achieved when the $G_r > 3$. This research has contributed to the field of system modeling and system identification. This research has contributed to the field of system modeling, system identification, and system stability analysis. This is a relatively new area that has a growing importance in control problems. The precise mathematical models are essential during the controller designing process because they allow the designer to estimate the closed-loop behavior of the plant. The errors in parameter values could result in poor instability and control. Therefore, adequacy and accuracy of parameters identification are primary modeling problems that always have to be addressed.

Table of Contents

Declaration	ii
Dedication	iii
Abstract	iv
List of Acronyms and Abbreviation	xii
List of Symbols	xiv
Acknowledgements	xvi
1 Introduction	1
1.1 Background of the Study	1
1.2 Definition of Terms	4
1.2.1 Electricity Generation	4
1.2.2 Motor	4
1.2.3 Alternator	5
1.2.4 Torque	5
1.2.5 Gear Ratio	5
1.2.6 Transfer Function	6

1.3	Statement of the Problem	6
1.4	Objectives of the Study	7
1.5	Significance of the Study	8
1.6	Justification of the Study	8
2	Literature Review	10
2.1	Introduction	10
2.2	Sustainability and Reliability of Solar Energy	10
2.3	Development of the Motor-Gear-Alternator (MGA) System	13
2.4	Parameter Identification	15
2.5	Stability Analysis	17
3	Methodology	20
3.1	Introduction	20
3.2	Formulation of a Mathematical MGA Model	20
3.2.1	Laplace Transformation	20
3.2.2	Derivation of the System Equations	22
3.2.3	DC Motor-Gear-Alternator Model	22
3.2.4	The Physical Model for the DC Motor-Gear-Alternator	23
3.2.5	Schematic Representation of the System	23
3.2.6	Alternator Equations	28
3.2.7	Motor-Gear-Alternator Coupling	29
3.2.8	Simulation Diagram from the Transfer Function	31
3.3	Parameter Identification for MGA Model	37
3.3.1	Pasek's Method	37

3.3.2	Frequency Response Method	37
3.3.3	The Pseudo Inverse Method	38
3.3.4	Step Response Method	39
3.3.5	Procedure for Parameters Identification	39
3.3.6	How Simulink Parameter Estimation Software Works	40
3.4	Analysis of the MGA Model	41
3.5	Stability of the MGA Model	47
3.5.1	The Routh-Hurwitz Method	47
3.5.2	Nyquist Method	51
3.6	Suitable Range of the Gear Ratio for the MGA Model From the Bode Plot	55
4	Simulation, Testing, Discussion and Results	58
4.1	Introduction	58
4.2	Description of the DC Motor-Gear-Alternator Simulink Model.	58
4.3	System Parameters	59
4.3.1	Data Estimation	60
4.3.2	Definition of Variables to be Estimated	62
4.3.3	The Estimation Task of Parameters	63
4.3.4	Viewing the Results	63
4.4	Analysis of MGA model	66
4.5	Open Loop Stability Analysis of The System	70
4.6	Closed Loop Stability Analysis	71
4.7	Gear Ratio Gain	71
4.8	Bode Diagram	72

5 Conclusion, Contributions and Recommendations	77
5.1 Conclusion	77
5.2 Contributions	78
5.3 Recommendation and Future Work	79
References	80
References	80
Appendices	85

List of Tables

Table 3.1	<i>System Specification</i>	46
Table 3.2	<i>Routh-Hurwitz Criterion</i>	49
Table 3.3	<i>Array of Coefficients</i>	51
Table 4.1	<i>Parameter Estimation Results</i>	66
Table 4.2	<i>Table of Different Values of PID Parameters</i>	70
Table 4.3	<i>Routh's Table</i>	70
Table 4.4	<i>Phase Margin and Gain Margin of the Different Values of the Gear Ratio</i>	73
Table 4.5	<i>Motor Specification</i>	74
Table 4.6	<i>Alternator Specification</i>	75

List of Figures

Figure 1.1	Transfer Function (Koech et al., 2016).	6
Figure 3.1	Physical Model for the DC Motor-Gear-Alternator (Koech et al., 2016).	23
Figure 3.2	Schematic Representation of the DC Motor-Gear-Alternator (Koech et al., 2016).	24
Figure 3.3	DC Motor model (Koech et al., 2016).	24
Figure 3.4	Alternator Model (Koech et al., 2016).	28
Figure 3.5	Motor-Gear-Alternator Coupling (Koech et al., 2016).	30
Figure 3.6	Signal Flow Graph Representation of Equation (3.33)(Author).	35
Figure 3.7	Simulation Diagram in State Variable Representation (Au- thor).	36
Figure 3.8	Observer canonical form (Author).	36
Figure 3.9	The Effect of Varying Damping Ratio on a 2nd Order System (Alciatore, 2007).	43
Figure 3.10	Typical 2 nd Order Step Response (Vaishnav and Khan, 2007).	45
Figure 3.11	Single Loop Feedback Control System (Author).	52
Figure 3.12	Cauchys Principle of Argument (Author).	54
Figure 3.13	Contour in the S-Plane (Author).	54
Figure 3.14	Bode Plot of Simple Pole (Mandal, 2006).	56

Figure 4.1	Block Diagram of DC Motor-Gear- Alternator System. (Koech et al., 2016).	59
Figure 4.2	Voltage Response of the Model Using the Initial Parameter Values.	60
Figure 4.3	Expected Response of the MGA.	61
Figure 4.4	Selecting Parameters for Estimation.	62
Figure 4.5	Selecting Which Parameters to Adjust in this Estimation.	63
Figure 4.6	Initial Voltage Response for the Actual and Estimated Models.	64
Figure 4.7	Voltage Response for the Experimental Data and Estimated Models.	65
Figure 4.8	Trajectories for Parameters.	65
Figure 4.9	Response of the MGA Model.	67
Figure 4.10	Unity Feedback System (Visioli, 2001).	68
Figure 4.11	Simulink Block with PID Controllers.	68
Figure 4.12	Step Response: (a) Response Without Controller (b) Response With Proportional Controller (c) Response With Integral Controller (d) Response With Derivative Controller.	69
Figure 4.13	Nyquist Plot for the System.	71
Figure 4.14	Step Response of the System for Different Values of Gear Ratio.	72
Figure 4.15	Nyquist Plot for Specified Values of Gear Ratio.	74
Figure 4.16	Graph of Gear Ratio against Alternator frequency.	75
Figure 4.17	Graph of Excess Voltage (v) against Gear Ratio.	76

List of Acronyms and Abbreviation

AC	Alternating Current
CO_2	Carbon (IV) oxide
DAQ	Data Acquisition
DC	Direct Current
DQ	Direct Quadrate
DS	Direct Synthesis
EMF	Electromotive Force
FESS	Flywheel Energy Storage System
GD	Gradient Descent
GUI	Graphical User Interface
LHP	Left Hand Plane
MATLAB	MATrix LABoratory
MGA	Motor-Gear-Alternator
NLS	Non Linear Least Square
ODE	Ordinary Differential Equation
PID	Proportional Integral Derivative
PM	Phase Margin
PMSM	Permanent Magnet Synchronous Machine

PO	Percentage Overshoot
PS	Pattern Search
SEIG	Self Excited Induction Generator
SISO	Single Input Single Output

List of Symbols

B_a	Viscous friction coefficients of the alternator
B_m	Viscous friction coefficients of the motor
i_a	Alternator current
i_m	Motor current
J_a	Moment of inertial of alternator
J_m	Moment of inertial of motor
K_a	Torque Constant of the alternator
K_m	Torque Constant of the motor
L_a	Inductance of the alternator
L_m	Inductance of the motor
R_a	Armature Resistance of alternator
R_m	Armature Resistance of the Motor
τ_a	Torque of alternator
τ_m	Torque of motor
V_a	Alternator Voltage
V_m	Motor Voltage
θ_a	Angular displacement of alternator
θ_m	Angular displacement of motor

ω_a Alternator angular velocity

ω_m Motor angular velocity

Acknowledgements

First and above all, I praise God, the almighty for providing me this opportunity and granting me the capability to proceed successfully. This thesis appears in its current form due to the assistance and guidance of several people. I would therefore like to offer my sincere thanks to all of them.

I would like to thank my supervisor, Prof. Samwel Rotich, for the patient, guidance, encouragement and advice he has provided throughout the research period. I have been extremely lucky to have a supervisor who cared so much about my work, and who responded to my questions so promptly. I am also indebted to my supervisor Dr. Titus Rotich who has been a constant source of encouragement, his willingness to help, unrivalled professional guidance and enthusiasm, not only during this thesis project but also during the two years of my PhD course work program. Special thanks go to my supervisor Dr. Fredrick O. Nyamwala for his constructive criticism and assistance in ensuring that this work met the desired standard and for his constant encouragement. It is through their selfless efforts that I successfully managed to accomplish the goal of this study.

I am grateful to Moi University, School of Biological and Physical Sciences for giving me the opportunity, facilities, resources and great research environment that allowed me to pursue my doctorate studies. I am also grateful to the funding received through partial scholarship and research fund to undertake my PhD.

Finally, my dearest wife Lornah, who led me through the valley of darkness with light of hope and support, my beloved kids: Eusley, Euginia, Eubyshev and Peasley who prayed for me and encouraged me throughout the period of my research. I warmly thank and appreciate my parents and my parents-in-law for their spiritual support in all aspects of my life.

Chapter 1

Introduction

1.1 Background of the Study

The world continues to move towards the renewable sources of energy. The majority of energy needs had been drawn from fossil fuels and other carbon fuels. Apart from the fact that fossils and other carbon fuels are obviously non-renewable, they release significant quantities of carbon emissions on use. The energy industry around the world strives to develop sustainable and reliable renewable energy systems. Solar energy is the primary point of focus (Martin & Rice, 2012). It is less practical and challenging to connect all households in the world to the national grid systems. The national grid extension programs are largely unsustainable and inefficient for countries to fulfill the targets to universal electricity access (Moner-Girona, Bódis, Huld, Kougias, & Szabó, 2016). Several parts of the world receive significant levels of sun cover. This study intends to support the off-grid electrification strategies due to elevated reliability and efficiency of the solar power.

The governmental, non-governmental and private organizations seem to consider strategies to attain a sustainable energy shift from carbon fuel technology to the

clean and sustainable energy. Besides, renewable energy sources can readily offer energy demands that are at the moment supplied by the non-renewable energy supply. Renewable energy systems will create job and provide security, sustainable development, commercial opportunities, and minimization of global warming (Tükenmez & Demireli, 2012).

The world's electricity usage in 2003 was approximately 7 TeraWatt-hours (TWh) and in 2007 was 12 TWh (Pérez-Lombard, Ortiz, & Pout, 2008). The demand for electricity is growing rapidly and the prediction for the year 2018 estimates the consumption to be 18 TWh and for 2030 a remarkable 25 TWh (Pérez-Lombard et al., 2008). On the other hand, the prevention of climatic change is considered as one of the most important international goals in energy policy. In the future, CO_2 emissions should desirably be lower than the current rates. CO_2 emission cuts seem practically difficult without the optimal usage of renewable natural resources of energy and reduction in the use of carbon fuels (Ayres, Bergh, Lindenberger, & Warr, 2013).

A different study placed the globe energy consumption rate at 10 TWh in 2006 and predicted the 2050 rate as 30 TWh. The world needs to draw 20 TWh of electricity from renewable sources in order to stabilize atmospheric CO_2 levels by 2050 (Razykov et al., 2011).

Electromechanical power amplification systems that employ alternators, gears and motors will play a crucial role in energy production and consumption. Therefore, the enhancement of the alternators and motors efficiencies is significant in the attempts to combat climate change and elevate efficiency in energy use. The permanent magnet energy systems are some of the developed models employed in the

design and manufacture of alternators and motors. The electromechanical power-conversion systems are founded on permanent-magnet technology. The permanent magnets are unavoidable when energy efficiency in energy generation and motoring are taken into consideration (Aleksashkin, Mikkola, et al., 2008).

The permanent magnets made it probable to develop novel energy conversion systems for competitive distribution of electricity. The enormous direct-driven windmill generators are a good example of the efficient use of permanent magnets. However, further research on the permanent magnet technology is necessary for further improvements and expansion of its usage (Aleksashkin et al., 2008).

The permanent magnetic materials have found an ever expanding industrial and domestic use since the innovation of the first generation carbon steel permanent magnets on the early times of the 20th Century. The permanent magnet based on motors are the popular type of linear and rotating electric machines applied in both generating and motoring modes. The machines that are based on the permanent magnet technology have been used for years in various applications where a low initial cost and simplicity of structure are of primary importance. In the recent times, the permanent magnet systems have been employed in more demanding applications. In the overall, the modern permanent magnet tools are competitive both in cost and performance with various machines (Aleksashkin et al., 2008).

The ideal rotor configuration, the mechanical design, the rotor electromagnetic and the stator electromagnetic design should be matched to attain a highly efficient system of the preferred load characteristics, high efficiency, high power factor and performance (Rizk & Nagrial, 2000).

Motor driven alternator works due to the fact that an alternator produces current when rotated. At the same time, a motor produces motion when an electric current passes through it. The two devices depend on each other for the production of an electric current.

1.2 Definition of Terms

1.2.1 Electricity Generation

The electricity generation is the practice of producing electricity from various sources of energy (Wu, Dai, Man, & Luo, 2012). The turbines are utilized to turn the magnets inside an electric generator. The kinetic energy is employed to spin the turbines; whereas the kinetic energy is derived from various sources since the power plants generate power out of different strategies such as hydropower, nuclear energy, wind power, thermal power, and fossil fuels (Wu et al., 2012). The fundamental principles of electricity generation were discovered during the 1820s and early 1830s by the British scientist Michael Faraday. His basic technique remains relevant to date. The power is produced by the rotation of copper disc, or a loop of wire between the poles of a magnet (Wu et al., 2012).

1.2.2 Motor

A motor is an electrical system, which transforms electrical energy into mechanical energy (Shumway-Cook & Woollacott, 2010). The original electric motors were based on electrostatic technology that was developed by a Scottish monk, known as Andrew Gordon in 1740s. The theoretical foundation surrounding the initiation of the mechanical force as a product of the interactions between the magnetic field

and the electric currents, Amperes force law, was developed later by Andr-Marie Ampere in 1820 (Beaty & Kirtley, 1998).

1.2.3 Alternator

An alternator is an electrical generator that produces alternating current (Bell & Åström, 1987). Dynamos were the first electrical generators capable of delivering power for industry, and the foundation upon which many other later electric power conversion instruments were developed. It included the alternating current alternator, the electric motor, and the rotary converters. Nowadays, the simpler alternator leads the large-scale power generation industry due to their high efficiency, cost effectiveness and reliability (Bell & Åström, 1987).

1.2.4 Torque

The torque is the determination of the tendency of a given force to spin an object about it's axis(Vas, 1998). It is denoted by τ and is defined as ;

$$\tau = \mathbf{F} \times d, \quad (1.1)$$

where \mathbf{F} is the Force in newtons, and d is distance in meters.

1.2.5 Gear Ratio

The gear ratio, G_r is the ratio of the number of teeth on the output gear (the one connected to the alternator) to the number of teeth on the input gear (attached to the motor) (Vas, 1998). The gear train is a system or a set of gears that are organized to transfer revolving torque from one region of the mechanical system to another. Since motors that are characterized by high torque and low rotational

speeds are usually used in control systems, the gear train is regularly adopted to elevate the revolving speed and lower the torque. The gear ratio represents the proportion of the output frequency with respect to the input frequency.

1.2.6 Transfer Function

The transfer function is associated with the system elements only and is not dependent on the excitation and initial conditions. The transfer function of a system (or a block) is defined as the ratio of output to input as shown in Figure 1.4

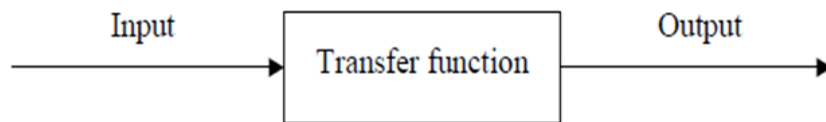


FIGURE 1.1: Transfer Function (Koech et al., 2016).

1.3 Statement of the Problem

It is nearly impossible to overstate the threat of climate change. Greenhouse gas emissions are rising more rapidly than predicted, and consequently, the world is warming more quickly. Global warming will have catastrophic effects such as accelerating sea level rise, droughts, floods, storms and heat waves. These will impact some of the world's poorest and most vulnerable people, disrupting food production, and threatening vitally important species, habitats, and ecosystems. The rapid increase in population, increasing technological activities and industrial advancement with respect to the small amount of energy generated in the country drives the desire to develop various effective energy generation models. It puts the researchers on the generating utility to employ technologies which efficiently supply power to the consumer.

Power cuts are common events and even small outages can have disastrous effects on unprepared businesses. Power failures are particularly critical at sites where the environment and public safety are at risk. Climate change, demand for electricity, pollution, and frequent power blackout are significant problems which need to be addressed.

1.4 Objectives of the Study

General Objective

The main objective of this study was to formulate a mathematical model describing the dynamics of a Motor - Alternator set coupled through a gear train, to produce enough energy to maintain the steady state and excess for additional loading.

Specific Objectives

The specific objectives of this study were to;

- (i) Estimate effective parameters of the Motor-Alternator Model.
- (ii) Analyze the MGA model using transient response.
- (iii) Determine the stability of the model using Routes Hurwitz and Nyquist criterion.
- (iv) Compute the suitable range of the gear ratio where stability is guaranteed from the bode plot.

1.5 Significance of the Study

A mathematical model is a description of a system using mathematical concepts and language. The model helps to explain a system and to study the effects of different components, and to make predictions about behaviour. The mathematical model developed is of great importance in the natural sciences and engineering disciplines. In many cases, the quality of a scientific field depends on how well the mathematical models developed on the theoretical side agree with results of repeatable experiments. This study designed a model which can be used by engineers or physicists to assemble the various components of the actual system or to control the system to satisfy a performance specification.

1.6 Justification of the Study

Solar energy is one of the sources of clean energy. Solar energy can support the off-grid electrification strategies by availing power to remote parts of the world. However, the current solar systems need substantial improvement in terms of efficiency, sustainability, and reliability (Moner et al., 2016). Besides, the current world's forest cover does not match the increasing fossil fuel consumption; hence, increased carbon (IV) emissions. Forests are an excellent carbon sinks. Deforestation due to expansion of agricultural activities and settlements coupled with increased carbon fuel use offsets balance between carbon emissions and capacity of carbon sinks to absorb CO_2 (Pan et al., 2011) . In this study, a Motor-Gear-Alternator prototype is designed to help enhance the power generator from solar energy direct current into an alternating current.

Climate change induced by increasing carbon (IV) oxide (CO_2) emissions caused

by economic development is a serious challenge. Substantial efforts are required to limit the concentration of CO_2 to a level that avoids critical temperature increases and the subsequent dramatic effects on economic performance, welfare, and ecosystems. The enticement to utilize 100 % energy from renewable sources has been motivated by the global warming phenomenon and various socioeconomic and ecological concerns (Pan et al., 2011).

The use of green energy is useful in leading the developments of the human societies by supporting attempts in establishment of sustainable environmental practices. In the industrialized world, the development of energy resources has become essential for transportation, agriculture, communications and waste collection to the extent that it is a prerequisite for development of any society. This study was important for societal development as well as in engineering and industrial advancement.

Chapter 2

Literature Review

2.1 Introduction

The developments of Motors and Generators or alternators have attracted a number of researchers in the past. The systems under study can be modeled and simulated using MATLAB or Simulink and ODE solvers. A few of the studies conducted on Motors and Generators or alternators by the researchers are reviewed in this chapter.

2.2 Sustainability and Reliability of Solar Energy

The world's energy industry is moving steadily into the establishment and development of renewable sources of energy (Rice & Cutler, 2012) . The solar power market was expanding at the rate of 35% to 40 % in the year 2011 (Razykov et al., 2011) . For instance, the Australian Government targets to draw at least 20 % of her total energy needs from the renewable energy supply by the year 2020. It is evident that renewable energy sources are less exploited and used compared with carbon fuels. Renewable sources of energy seem to face socio-technical barriers,

barriers in financial incentives, policies, and infrastructure issues. Australia seems to lack behind in renewable energy system installation capacity and generation; the observation may apply to other countries (Rice & Cutler, 2012).

Solar energy is a good alternative for the realization of universal access to electricity. Many people in the world have no access to power supply. In Burkina Faso, about 95 % of the rural population do not have access to electricity. Still, in the same country, the national power grid seems unsustainable and inefficient. The situation presents a challenge in the strategies intended to limit the demand and consumption of fossil fuels (Moner et al., 2016). In the same study, (Moner et al., 2016) pointed out that Burkina Faso will need to increase the use of fossil fuels in order to expand the national grid. The approach will be on the contrary to global strategies aimed at the reduction of carbon (IV) oxide emissions. The country currently generates an estimated 70 % of her energy needs from the thermal-fossil fuels. Burkina Faso has constructed a total of 28 fossil fuel power plants and 4 hydroelectric stations (Moner et al., 2016).

The world's forests are one of the largest carbon sinks. Nevertheless, the forest cover is slowly dropping amid challenges such as increased human population, high demand for agricultural and settlement areas and high rate of deforestation. In a study, the total forest carbon sink capacity was placed at 2.4 ± 0.4 pentagrams of carbon annually, at least as from 1990 to 2007. However, the current world forest cover does not effectively compensate for seemingly ever increasing carbon emissions (Pan et al., 2011). It is a narrow approach, to attribute the growing greenhouse emission solely to the use of carbon fuels. Livestock farms are known to release significant quantities of greenhouse gas pool into the atmosphere. The

anaerobic digestion results in the emission of greenhouse gasses such as methane and nitrous oxide. The gasses are released during digestion process as well as through the decomposition of organic manure. It is a challenge to place useful statistic on the extent of greenhouse gasses generation from livestock on a global scale. However, computer simulation prototypes can be employed to estimate the scope of greenhouse emissions from livestock activities (Jose et al., 2016).

The solar energy generation technology has made substantial progress over the years. It includes the innovation and progressive development of the photovoltaic cells which are excellent alternatives for sustainable and reliable future energy requirements. However, the solar cell technology is yet to attain sufficiently high reliability and efficiency. The space program as from the 1950s may have increased the advancement of the photovoltaic cells since they were fitted on to satellites (Razykov et al., 2011) .

The car industry forecasts upsurge of electric vehicles on the roads in the years to come. Solar power may act as a primary source of power for electric vehicles. The electric car evolutionary change will include the development of solar cells that will drive vehicles for extended hours and thus covering long distances. The sales of electric vehicles will tend to increase per annum. The solar technology is characterized by a continuous incremental enhancement, improved performance and throughput, and release of a new generation of products (Orbach & Fruchter, 2011) . The MGA system can work in tandem with solar energy generation systems. In fact, solar cells can be placed on the building and car rooftops. The infrastructure and construction industry are accountable for 46 % of whole world energy consumption (Olsthoorn, Haghghat, & Mirzaei, 2016).

The solar energy varies wildly across regions and periods. However, the solar power technology continues to expand in terms of extending of market penetration and sales. The solar power resources need to be further improved in order to increase grid stability (Antonanzas et al., 2016).

The solar harvesting technology has advanced significantly over the last decade to the current times. However, the primary disadvantage associated with solar energy is that it is subject to varying power output with the deviation of solar irradiance and temperature fluctuations (Sudhakar et al., 2016).

2.3 Development of the Motor-Gear-Alternator (MGA)

System

Computer simulation systems have been widely employed to examine challenging practical phenomena. It includes the estimation of the quantities of greenhouse gas emission from the global livestock activities. The computer simulation models are often fast and efficient (Jose et al., 2016). The increasing energy demand across the world drives the exploitation and usage of renewable energy systems. Solar energy is an efficient and readily available renewable energy resource. The MGA model may enhance or maximize the conversion of DC solar power output into AC (Koech, Rotich, Rotich, & Nyamwala, 2016).

Pulsating torque is a critical problem associated with the surface-mounted permanent magnet based motors. Hence, the resultant torque is most often non-uniform (Roca & Duguleană, 2016). The issue will present a challenge during the development and testing of the functional MGA system. The problem can be corrected

using Proportional Integral Derivative (PID) controllers and designed in order to minimize periodic disturbances. However, the permanent magnet motors are associated with constant speed thus a steady current and voltage is generated. During the construction of the real system in the future, care must be observed so as to eliminate or reduce acoustic noise, shaft vibration, and damages to the moving components such as the gears (Roca & Duguleană, 2016).

Best matching and pairing gear teeth should be selected in order to reduce vibrations and tear or wear. Good fitting gears will help to minimize cogging torque. Some analysts proposed for the construction of new electric motor designs but the move will be expensive and time-consuming. Pole shifting is one of the strategies that will help in the minimization of cogging torque. In this approach, the magnetic poles are moved along the rotor circumference so as to compensate each other. It contributes to the reduction of total costs through a minimization of consumption costs (Roca & Duguleană, 2016).

It is reported that more than 90 % of the electricity around the world is produced through the utilization of electromagnets in accordance with the Faradays law of electromagnetic induction (Grover, Kumar, & Ramalla, 2014). The magnets influence a magnetic field, in such a way that the magnetic fields repel each other, thus, causing Electromotive Force (E.M.F) to be induced. The electricity generated was used to recharge a mobile battery. The amplification of voltage is necessary for commercial and domestic use.

In 2013, Niu designed and modeled a permanent magnet linear-synchronous generator. Two of the independent physical parameters of the generator were studied. The results indicated that there is potential for improvements of the permanent

magnet linear synchronous generator modeled in his work, as well as potential for improving the system model (Niu, 2013).

Electric machines comprising of magnets are employed to produce power that supplies mechanical machines in industries (Yusuf, Samosir, & Abdulkadir, 2012). The Simulink in MATLAB was employed because of its broad distribution. The results demonstrate the simulated wave-form of machine performance and speed, load torque and armature current which suits theoretical analysis (Yusuf et al., 2012).

It is mentioned that generator can be presented with a model of second, third, fifth, and seventh order. As the order grows, the model becomes more complex. Each model is used for testing and determination of different behaviors (Špoljarić, Miklošević, & Jerković, 2010) . A mathematical model of MGA is apparently important for analysis, control and monitoring purposes.

2.4 Parameter Identification

The primary goal is to identify system parameters through mathematical modeling to attain optimum design requirements. Parameter identification begins with the collection of relevant data with the support of the MATLAB system identification toolbox. The model estimation and validation tests are vital steps. The mathematical modeling strategy is a cheap and efficient method for study and representation of a physical system. The system identification procedure involves the following steps: the selection of parametric and non-parametric modeling techniques, the selection of model structure, and development of an estimation and validation criteria (Rabbani, Hussain, Ali, et al., 2013) .

The main purpose of most system parameter estimation is to develop a mathematical model that fully describes an underlying physical system which can be used to predict both the response of the system to disturbance and the design advantage which might be obtained from modification of the system (Mottershead & Friswell, 1993). This mathematical model can be used to explain the behavior of the system and to predict its response to various inputs at different conditions (Basilio & Moreira, 2004).

Methods to estimate model parameters from both open loop and closed loop step responses was proposed (Ahmed, Huang, & Shah, 2007). A number of methods for system parameter estimation (Ahmed et al., 2007), (Box, Jenkins, Reinsel, & Ljung, 2015), (Cluett & Wang, 1991), (Marquardt, 1963), (McFadden, 1989) and (Tarantola, 2005) can be applied to MGA model identification. In particular, various methods have been used by many researchers to estimate parameters of models; that is, (Fliess & Sira-Ramirez, 2008), (Mamani, Becedas, Feliu-Batlle, & Sira-Ramirez, 2007) and (Mamani, Becedas, Feliu-Batlle, & Sira-Ramírez, 2008) used the algebraic identification techniques, (Liu, Xie, & Ding, 2009) used a recursive least-squares parameter estimation algorithm for non-uniformly sampled multirate systems, (Tarantola, 2005) used an inverse problem theory and methods for model parameter estimation, (Marquardt, 1963) applied an algorithm for least-squares estimation of nonlinear parameters and (McFadden, 1989) used a method of simulated moments for estimation of discrete response models without numerical integration.

The present study proposed a new method of parameter estimation using Simulink parameter estimation tool via step response methodology.

2.5 Stability Analysis

The idea of stability of systems is of fundamental importance and from an application perspective, an unstable system is of no importance. It implies that the system may blow-up while active. One of the most useful tasks a control engineer is needed to do, in relation to the design and the analysis of control systems, is to guarantee its stability. The stability of a linear model can be investigated by Nyquist Diagram, Routh-Hurwitz, Bode Diagram, and the methods of the Lyapunov (Nelles, 2013).

The transfer functions representation is particularly important when analyzing system stability (Silverman & Anderson, 2012). If all poles of the transfer function (given that the values of s in which the denominator is equivalent to zero) have negative real components, then the system is stable. If any pole has a positive real element, then the system is unstable. If the poles are positioned on the complex s -plane, then all the poles should be in the Left Half of the Plane (LHP) to guarantee stability. If any pair of poles lies on the imaginary axis, the system is marginally steady and the system will oscillate. The poles of a model can easily be determined in MATLAB by employing the pole command.

Stability analysis supports the planning and running of power systems. The accuracy of the stability estimation procedures is subject to identified parameters and model structures of the power system elements. In essence, precise parameter values should be determined (Saavedra-Montes, Ramos-Paja, & Ramírez, 2012).

The Nyquist criterion is described as a graphical approach, which allows for the determination of the stability of a given closed-loop model from the open-loop

transfer function. The frequency can range from the zero to infinity (Goldstein & Soltan, 2000).

The stability analysis utilizing the Nyquist strategy allows the system designers to obtain improved performance from their circuits. System design includes the consideration of specifications such as power efficiency, linearity, and stability over a broad range of input power and impedance. The circuit stability can be calculated from the s-domain of a given active system, output and input matching circuits (Goldstein & Soltan, 2000).

The frequency domain stability determination developed by Nyquist H. in 1932 has remained a fundamental strategy to the examination of stability of linear models (Nyquist, 1932). The stability criterion demonstrated by Nyquist is dependent on the theorem of Cauchy regarding the mapping of contours in the complex plane. The Nyquist model is a semi-graphical method that regulates the stability of the closed-loop system by assessing the properties of the frequency domain plot of the closed-loop transfer function $G(s)H(s)$.

The Nyquist stability criterion (Balabanian & Lepage, 1956), (Bode et al., 1945) and (James, Nicholas, & Phillips, 1947) offers a simple graphical method for determining the closed-loop stability from the frequency-response graphs of the open-loop transfer formula $G(s)H(s)$.

The stability of the MGA system may be studied using the Nyquist strategy. By employing the Cauchy's theory of argument to the open-loop model of transfer function, the author got information about the stability of the closed-loop model of transfer function and obtained the Nyquist stability criterion. The significance of Nyquist stability depends on the fact that it may also be utilized to determine

the relative rate of model stability.

Barmish (2004), described the Hurwitz property for polynomials with perturbed coefficients. Given a strictly Hurwitz polynomial;

$$f(\lambda) = \lambda^n + a_{n-1}\lambda^{n-1} + a_{n-2}\lambda^{n-2} + a_1\lambda + a_0 \quad (2.1)$$

it is of interest to know how much the coefficients a_i , $i=1,2,\dots,n-1$ can be perturbed while simultaneously preserving the strict Hurwitz property (Barmish, 1984).

Based on this protocol, in this work the Mathematical model was developed by a detailed mathematical derivation from first principles, and represented the derived equations within Simulink. The effect of each of the Proportional, Integral and Derivative (PID) controllers on the closed-loop system was discussed and demonstrated how to utilize a PID controller to advance the system performance. The step response has also been used to analyze the transient behavior of the MGA system. Finally, the stability of both the open-loop and the closed-loop control systems using Routh-Hurwitz, Nyquist criterion, and Bode plot was presented.

Chapter 3

Methodology

3.1 Introduction

This chapter addresses the mathematical tools and methods used extensively for the design and analysis of the MGA model. The goal is to study and derive a suitable linear model to represent MGA dynamics to be used for control design. Formulation of the MGA model is presented in Section 3.2, parameter estimation for the MGA model is described in Section 3.3, Section 3.4 shows the analysis of the MGA model using transient response. Section 3.5 presents stability of the MGA model using Routh's Hurwitz and Nyquist criterion. Finally, Section 3.6 studies the suitable range of the gear ratio of the MGA model from the Bode plot.

3.2 Formulation of a Mathematical MGA Model

3.2.1 Laplace Transformation

The telegraph equation founded in 1880 by Oliver Heaviside is employed extensively in Engineering and Science. The applications include analysis of electri-

cal signals, designing and modeling of the reaction diffusion. The equation frequently appears in Fluid Dynamics, Electro-chemistry, Mathematical Biology, and Physics and can be solved through different strategies. It includes Fourier transform, Laplace transform and the combined Fourier-Laplace transform (Dhunde & Waghmare, 2016). In this case, the Laplace transformation was applied to analyze the electrical signals for the MGA model.

The Laplace transform could be employed without opting for the domain decomposition strategies. The transform can be computed through differentiation of the original equations or be solved through integration by parts (Belgacem & Silambarasan, 2013). Integral transforms are of great significance in various fields of science in which the Laplace transform can be applied to solve non-linear and linear ordinary or partial differential equations (Alshikh, 2016)(Gardner, 1942). Through the utilization of Laplace transform, tasks like integration and differentiation can be replaced by algebraic processes such that, a linear differential equation can be altered into an algebraic equation in a complex variable s . The method is simple and efficient. (Belgacem & Silambarasan, 2013).

The Laplace transform is a mathematical modeling tool utilized for the description, analysis and simulation of various systems through the recruitment of ordinary differential equations (Wójcik, Szukiewicz, & Kowalik, 2014). The approach is advantageous compared with the decomposition since it can solve nonlinear problems without employing the domains polynomials (Kumar, Singh, & Rathore, 2012).

The design and analysis of a linear system are also worked-on in the s -domain without really solving the differential equations relating to the dynamics of the system. The graphical approaches such as the Bode plot and Nyquist Diagram

utilize the Laplace transform strategy for assessment of the system performance. In addition, the transient response and the steady-state reaction of a dynamical system can be achieved by the Laplace transform method.

3.2.2 Derivation of the System Equations

The mathematical description of DC Motor-Gear-Alternator is modeled on the following assumptions:

- (i) The eddy currents associated with iron are not taken into account.
- (ii) The mass of the rotary damper is assumed to be negligible.
- (iii) The energy supplied to the DC motor is constant.
- (iv) Losses due to the simple mechanical friction and heating are negligible.

3.2.3 DC Motor-Gear-Alternator Model

To model the MGA system, the steps are as follows;

- (i) Developing a physical model for the DC Motor-Gear-Alternator.
- (ii) Schematic Representation of the system.
- (iii) Derivation of system equations from the first principle.

(iv) Analyze the model to assess its performance by using available mathematical tools.

(v) Study stability of the system for practical applications.

3.2.4 The Physical Model for the DC Motor-Gear-Alternator

The physical prototype for the DC Motor-Gear-Alternator is as shown in Figure 3.1. The motor and the alternator components of the system were assembled as

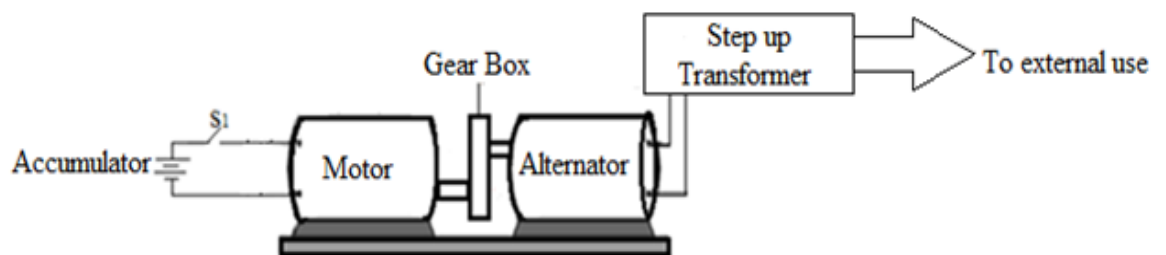


FIGURE 3.1: Physical Model for the DC Motor-Gear-Alternator (Koech et al., 2016).

shown in Figure 3.1 above. The gear element was introduced in between the motor and the alternator components as an amplifying system. The intensification of power by the gear unit necessitates the establishment of the relationship between the gear ratio, the input power, and the power output. It is primarily made possible by developing a mathematical model incorporating this correlation.

3.2.5 Schematic Representation of the System

The diagram of Figure 3.2 is a schematic representation of the Motor- Gear- Alternator set components. The mathematical model for DC Motor-Gear-Alternator is found using Kirchhoffs voltage law (Kish, 2006), ohms law (Urone & Hinrichs,

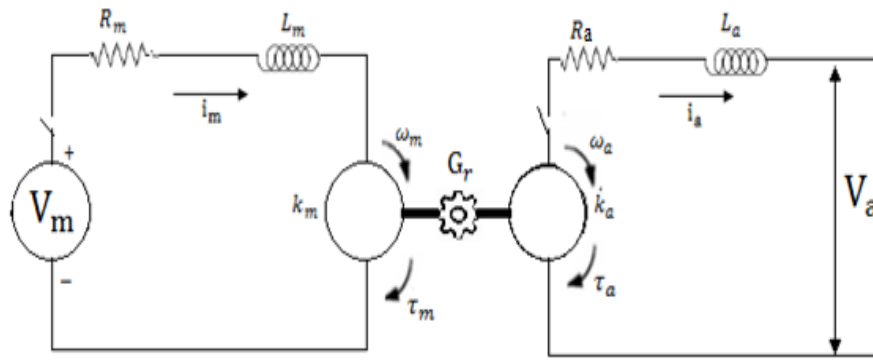


FIGURE 3.2: Schematic Representation of the DC Motor-Gear-Alternator (Koech et al., 2016).

2016) and Newton's second law of motion (Bejan, 2016). The electric circuit of the motor is shown in Figure 3.3.

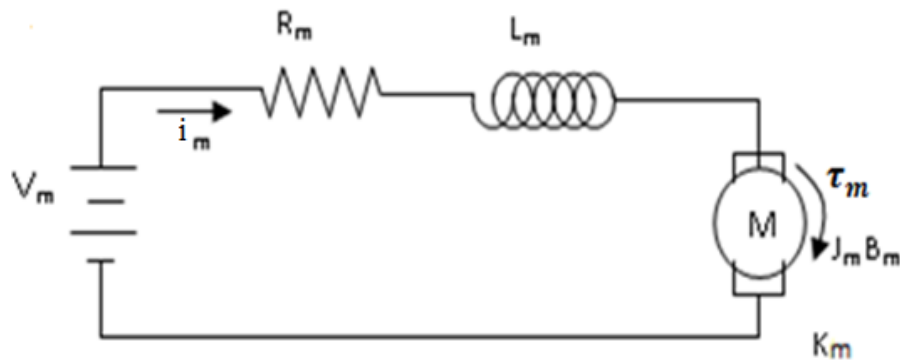


FIGURE 3.3: DC Motor model (Koech et al., 2016).

In a more general case, inductance is defined as

$$L = \frac{d\phi}{di}, \quad (3.1)$$

where L represents inductance, i is the electric current and ϕ is the magnetic flux. Any change in the current via an inductor develops a changing flux, thus, inducing a voltage across the inductor. In accordance with Faraday's Law of induction, the

voltage induced through any alteration in magnetic flux in the the circuit is,

$$V_1 = -\frac{d\phi}{dt} \quad (3.2)$$

From (3.1) above,

$$V_1 = -\frac{d}{dt}(Li) = -L\frac{di}{dt}. \quad (3.3)$$

The voltage , V , is proportional to the angular velocity of the shaft by a constant factor K_e

$$V_2 = K_e\omega, \quad (3.4)$$

Ohm's Law states that the current flowing via a conductor between two given points is directly proportional to the total voltage across the two points. Introducing the constant of proportionality, the resistance, mathematical equation that describes this relationship is,

$$V_3 = iR, \quad (3.5)$$

whereby i represents the current that flows through the conductor in amperes (A), V is the voltage measured across the conductor in volts (V), and R is the resistance of the conductor in ohms.

Applying Kirchhoffs voltage law to the motor, the following equation was obtained,

$$V_m = V_1 + V_2 + V_3, \quad (3.6)$$

or

$$V_m(t) = L_m\frac{di_m}{dt}(t) + K_e\omega_m(t) + R_m i_m(t), \quad (3.7)$$

and

$$i_m = \frac{\tau_m}{K_m}, \quad (3.8)$$

where, V_m is the motor voltage, R_m is the motor armature resistance, i_m is the Motor current, L_m is the inductance of the motor, K_e is the Torque Constant of the motor, ω_m is the motor angular velocity. τ_m is the torque of the motor.

Through the application of the Laplace transform with zero initial condition, the following equation was achieved

$$V_m(s) = L_m s \frac{\tau_m}{K_m}(s) + K_e \omega_m(s) + R_m \frac{\tau_m}{K_m}(s) + . \quad (3.9)$$

The uneven torque acting on the body along the rotational axis determined the rate of change of the systems angular momentum,

$$\tau = \frac{dl}{dt}, \quad (3.10)$$

where, t is the time in seconds and l is the angular momentum vector in kilogram metres squared per second .

For rotation about a fixed axis,

$$l = J\omega, \quad (3.11)$$

where, ω is the angular velocity in radians per second and J is the moment of inertia in kilogram metre squared. It followed from equation (3.10) that;

$$\tau_1 = \frac{dl}{dt} = \frac{d(J\omega)}{dt} = J \frac{d\omega}{dt}. \quad (3.12)$$

The frictional force is proportional to the object's velocity, v , giving the relationship $F = -Bv$, where B is the frictional drag. Relating this equation to rotational motion results in

$$\tau_2 = -B_m\omega_m. \quad (3.13)$$

Motor torque τ_m is proportional to the motor armature current i_m by a constant factor K_m as shown in equation (3.8),

$$\tau_3 = K_m i_m. \quad (3.14)$$

Applying Newton's second law of motion to the motor, the net torque developed by the motor is proportional to the rate of change of angular velocity as,

$$J_m \frac{d\omega_m}{dt} = K_m i_m - B_m \omega_m, \quad (3.15)$$

or,

$$K_m i_m = J_m \frac{d\omega_m}{dt} + B_m \omega_m, \quad (3.16)$$

therefore,

$$\tau_m = J_m \frac{d\omega_m}{dt} + B_m \omega_m, \quad (3.17)$$

where, τ_m is the torque of the motor, ω_m is the motor angular velocity, J_m is the moments of inertia of the motor and B_m is the viscous friction coefficients.

Through the application of the Laplace transform to equation (3.17) with a zero initial condition, the following equation was achieved,

$$\tau_m = J_m s \omega_m(s) + B_m \omega_m(s). \quad (3.18)$$

Substituting (3.18) into equation (3.9) the following equation was derived,

$$\frac{\omega_m}{V_m} = \left[\frac{K_m}{(R_m - L_m s)(J_m s + B_m) + K_m K_e} \right] \quad (3.19)$$

For this model K_m and K_e are equal. Therefore, the transfer function for the motor becomes

$$\frac{\omega_m}{V_m} = \left[\frac{K_m}{(R_m - L_m s)(J_m s + B_m) + K_m^2} \right] \quad (3.20)$$

3.2.6 Alternator Equations

Similarly, electric circuit of the alternator is shown in Figure 3.4. Applying Kirch-

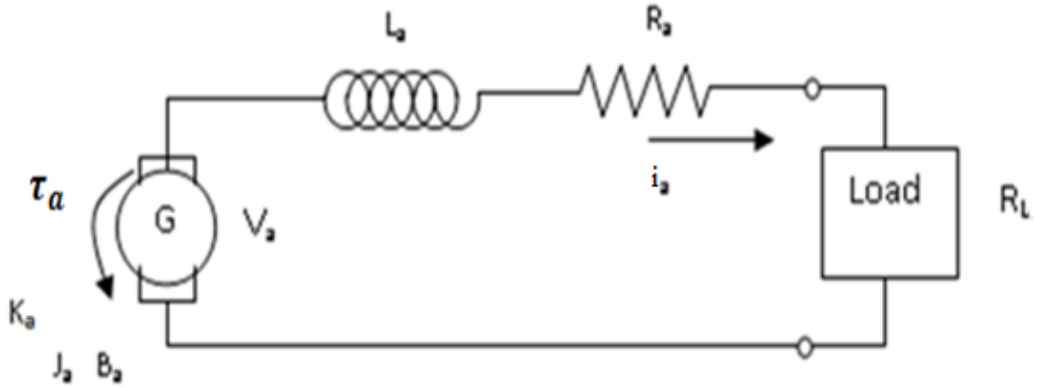


FIGURE 3.4: Alternator Model (Koech et al., 2016).

hoffs voltage law, the voltage definition of the alternator is similar to that of the motor, equation (3.7) but with alternator definitions as follows,

$$K_t \omega_a(t) = R_a i_a(t) - L_a \frac{di_a}{dt}(t) + V_a(t), \quad (3.21)$$

where , K_t is the shaft constant of the alternator, ω_a is the angular velocity of the alternator, R_a is the alternator resistance, i_a is the alternator current, V_a is the

alternator output voltage.

Substituting $i_a = \tau_a/K_a$ in equation (3.21) and taking Laplace transform, where τ_a is the alternator torque and K_a is the torque constant, the following equation was obtained,

$$K_t\omega_a(s) = R_a\frac{\tau_a}{K_a}(s) - L_a s\frac{\tau_a}{K_a}(s) + V_a(s) \quad (3.22)$$

Applying Newtons second law of motion, the net torque acting in the alternator is,

$$\tau_a(s) = J_a s\omega_a(s) + B_a\omega_a(s) \quad (3.23)$$

Through the Substitution of equation (3.23) into equation(3.22) , the following equation was obtained,

$$\frac{V_a}{\omega_a} = \frac{K_t K_a - (R_a - L_a s)(J_a s + B_a)}{K_a}. \quad (3.24)$$

For this model K_t and K_a are approximately equal. Therefore,(3.25)

$$\frac{V_a}{\omega_a} = \frac{K_a^2 - (R_a - L_a s)(J_a s + B_a)}{K_a}. \quad (3.25)$$

gives the transfer function for the alternator.

3.2.7 Motor-Gear-Alternator Coupling

Figure 3.5 is used to derive the relationship between voltage entering the motor, gear ratio and voltage leaving the alternator. The gears were introduced in between the motor and alternator for amplification purposes.

The gear ratio, G_r , expresses the ratio of the frequency of the motor shaft to the frequency of the alternator shaft. Thus, the investigator can multiply

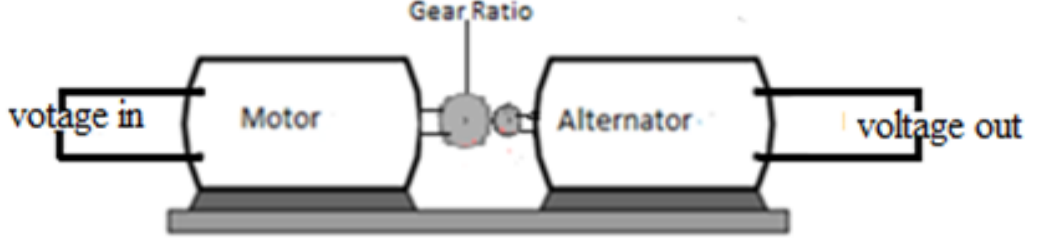


FIGURE 3.5: Motor-Gear-Alternator Coupling (Koech et al., 2016).

the frequency f_m of the motor shaft (the input) with the gear ratio to find the frequency f_a of the alternator rotor (the output). It was calculated as follows,

$$f_a = G_r f_m \quad (3.26)$$

The relationship between angular speed of the shaft and the frequency is given by

$$\omega = \frac{2\pi}{T} = 2\pi f, \quad (3.27)$$

where, ω represented the angular speed determined in radians per unit second, f is the ordinary frequency measured in Hertz, and T is the periodic time measured in seconds..

From equations (3.27) and (3.25), the following two relationships were obtained

$$\omega_a = 2\pi f_a = \left[\frac{V_a K_a}{K_a^2 - (R_a - L_a s_a)(J_a s_a + B_a)} \right], \quad (3.28)$$

and from equations (3.27) and (3.20)

$$\omega_m = 2\pi f_m = \left[\frac{K_m V_m}{(R_m - L_m s)(J_m s + B_m) + K_m^2} \right], \quad (3.29)$$

Using equations (3.26), (3.28) and (3.29), the following equation was obtained,

$$\left[\frac{V_a K_a}{K_a^2 - (R_a - L_a s)(J_a s + B_a)} \right] = G_r \left[\frac{K_m V_m}{(R_m - L_m s)(J_m s + B_m) + K_m^2} \right]. \quad (3.30)$$

Simplifying equation (3.30) with assumption that $K_m = K_a = K$, to obtain the equation,

$$\frac{V_a}{V_m} = G_r \left[\frac{K^2 - (J_a s + B_a)(R_a - L_a s)}{(R_m - L_m s)(J_m s + B_m) + K^2} \right], \quad (3.31)$$

or

$$G(s) = G_r \left[\frac{J_a L_a s^2 - (J_a R_a - B_a L_a) s - (B_a R_a - K^2)}{-J_m L_m s^2 + (J_m R_m - B_m L_m) s + (B_m R_m + K^2)} \right]. \quad (3.32)$$

Where $G(s)$ is transfer function and equation (3.32) is the Mathematical model of DC Motor-Gear-Alternator Model.

3.2.8 Simulation Diagram from the Transfer Function

The author presented one method for deriving a simulation diagram from the transfer function. Since the state-variable representation is not unique, there are, theoretically, an infinite number of ways of writing the state equations. An analogous process may be observed for writing the discrete-state equation from the transfer functions. The transfer functions of the single-input-single-output system of the form:

$$G(s) = \frac{a_n s^n + a_{n-1} s^{n-1} + \dots + a_1 s + a_0}{b_n s^n + b_{n-1} s^{n-1} + \dots + b_1 s + b_0}, \quad (3.33)$$

where, $a_i, b_i ; i = 0, 1, 2 \dots n$ are constant coefficients of the polynomial in s . It may be written, after introducing an auxiliary variable $E(s)$, as:

$$G(s) = \frac{(a_n s^n + a_{n-1} s^{n-1} + \dots + a_1 s + a_0) E(s)}{(b_n s^n + b_{n-1} s^{n-1} + \dots + b_1 s + b_0) E(s)} = \frac{Y(s)}{U(s)}, \quad (3.34)$$

where

$$Y(s) = (a_n s^n + a_{n-1} s^{n-1} + \cdots + a_1 s + a_0)E(s) \quad (3.35)$$

is the Laplace transform of $y(t)$ and

$$U(s) = (b_n s^n + b_{n-1} s^{n-1} + \cdots + b_1 + b_0)E(s) \quad (3.36)$$

is the Laplace transform of $u(t)$.

The following relationships were obtained among the variables in the time domain and s domain with zero initial conditions

$$\begin{aligned} E(s) &\rightarrow e(t) \\ sE(s) &\rightarrow \dot{e}(t) \\ s^2 E(s) &\rightarrow \ddot{e}(t) \end{aligned} \quad (3.37)$$

From equation (3.37) the state variables $x_i(t)$, $i = 1, 2, \dots, n$ are defined as,

$$\begin{aligned} x_1(t) &= e(t) \\ x_2(t) &= \dot{x}_1(t) = \dot{e}(t) \\ x_3(t) &= \dot{x}_2(t) = \ddot{e}(t) \\ x_n(t) &= \dot{x}_{n-1}(t) = e^{n-1}(t) \end{aligned} \quad (3.38)$$

From equations (3.38) the state equations are obtained as;

$$\begin{aligned}
 \dot{x}_1(t) &= x_2(t) \\
 \dot{x}_2(t) &= x_3(t) \\
 \dot{x}_3(t) &= x_4(t) \\
 \dot{x}_n(t) &= [-b_0x_1(t) - b_1x_2(t) - b_2x_3(t) \cdots - b_{n-1}x_n(t)]/b_n + u(t) \quad (3.39)
 \end{aligned}$$

This leads to

$$\begin{bmatrix} \dot{x}_1 \\ \dot{x}_2 \\ \dot{x}_3 \\ \vdots \\ \dot{x}_n(t) \end{bmatrix} = \begin{bmatrix} 0 & 1 & 0 & \cdots & 0 \\ 0 & 0 & 1 & \cdots & 0 \\ 0 & 0 & 0 & \cdots & 0 \\ \vdots & \vdots & \vdots & \vdots & \vdots \\ -b_0/b_n & -b_1/b_n & -b_2/b_n & \cdots & -b_{n-1}/b_n \end{bmatrix} \begin{bmatrix} x_1(t) \\ x_2(t) \\ x_3(t) \\ \vdots \\ x_n(t) \end{bmatrix} + \begin{bmatrix} 0 \\ 0 \\ 0 \\ \vdots \\ 1/b_n \end{bmatrix} u(t).$$

In compact form, it is written as

$$\dot{x}(t) = \mathbf{A}x(t) + \mathbf{B}u(t), \quad (3.40)$$

where, \dot{x} describes the continuous rate of change of the system, $x(t)$ is the current state of the system and $u(t)$ is the output of the system, \mathbf{A} and \mathbf{B} are $m \times n$ and $m \times r$ matrices of the constant coefficients a_{ij} and b_{ij} that describe the state variables and system input respectively.

The output of the system is the results obtained after running system variable of interest. A significant property of the linear state equation is that all variables of

the system can be represented by state variables x_i which is a linear combination and the inputs u_i . An output equation of order n with r inputs can be written as:

$$y(t) = c_1x_1 + c_2x_2 + \cdots + c_nx_n + d_1u_1 + d_2u_2 + \cdots + d_nu_n \quad (3.41)$$

where, the c_i and d_i are constants. If n variables are defined as outputs, the n equations take the same form as in equation (3.40) and may be written compactly as

$$\mathbf{y}(t) = \mathbf{C}x(t) + \mathbf{D}u(t), \quad (3.42)$$

whereby, \mathbf{y} is the output variables of $y_i(t)$, \mathbf{C} is a matrix of constant coefficients c_{ij} that describe the state variables, \mathbf{D} is a matrix of the constant coefficients d_{ij} that describe the inputs of the system. For most systems, the matrix \mathbf{D} is the Zero matrix, and equation (3.42) reduces to a state variable:

$$\mathbf{y}(t) = \mathbf{C}x(t) \quad (3.43)$$

Equations (3.40) and (3.43) are a set of linear state and output equations respectively for the continuous system defined by higher-order system represented by transfer function of equation (3.33).

An alternative convenient and valuable representation of the continuous model is through the utilization of the signal flow graph or the comparable simulation diagram. These two forms may be derived, after multiplying the numerator and the denominator of the function (3.34) by s^{-n} ,

$$G(s) = \frac{Y(s)}{U(s)} = \frac{a_n + a_{n-1}s^{-1} + \cdots + a_1s^{1-n} + a_0s^{-n}E(s)}{b_n + b_{n-1}s^{-1} + \cdots + b_1s^{1-n} + b_0s^{-n}E(s)} \quad (3.44)$$

From this expression the following two equations were derived

$$Y(s) = (a_n + a_{n-1}s^{-1} + \dots + a_1s^{1-n} + a_0s^{-n})E(s) \quad (3.45)$$

$$U(s) = (b_n + b_{n-1}s^{-1} + \dots + b_1s^{1-n} + b_0s^{-n})E(s) \quad (3.46)$$

Equation (3.46) can be rewritten in the form

$$E(s) = U(s)/b_n - [-b_{n-1}s^{-1} - \dots - b_1s^{1-n} - b_0s^{-n}] \quad (3.47)$$

Equations (3.45) and (3.47) are used to draw the signal flow graph shown in Figure 3.6, whose transfer function is given by equation (3.33).

In signal flow graph the term $s^{-1} = \frac{1}{s}$ represents pure integration and $b_i, i =$

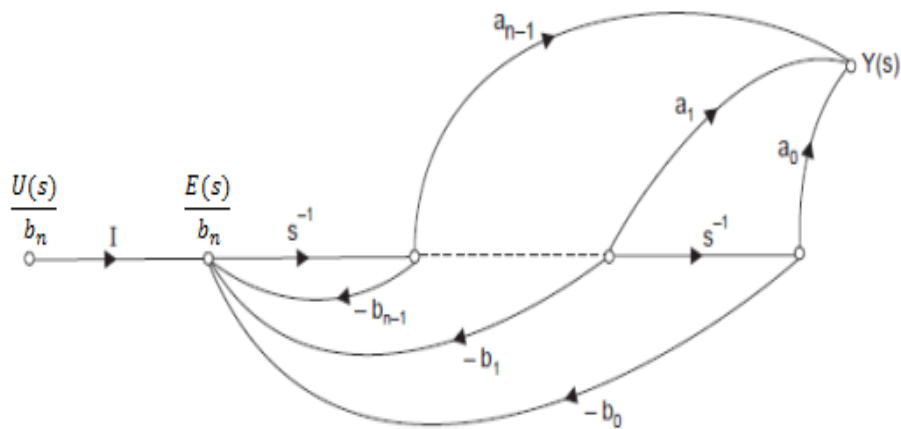


FIGURE 3.6: Signal Flow Graph Representation of Equation (3.33)(Author).

$0, 1, 2, \dots, n$ represent gain. The signal flow graph of Figure 3.6 can also be represented by the equivalent simulation diagram, with the states indicated as in Figure 3.7. Noting the structure of the signal flow graph in Figure 3.6 and its relationship to the numerator and denominator polynomials denoted by equations (3.45) and (3.46), It is ostensible that the simulation diagram or signal flow graph can be

achieved by review of the transfer function in equation (3.33). Given the condition that the signal flow graph is drawn from the state equation, the Mansons gain formula may be applied to find transfer function that demands the computation of inverse of a matrix (Sinha, 2008). The assembly of Figure 3.6, and the functions (3.45) and (3.46), is known as the phase-variable canonical form of model representation. A different standard form referred to as the observer canonical

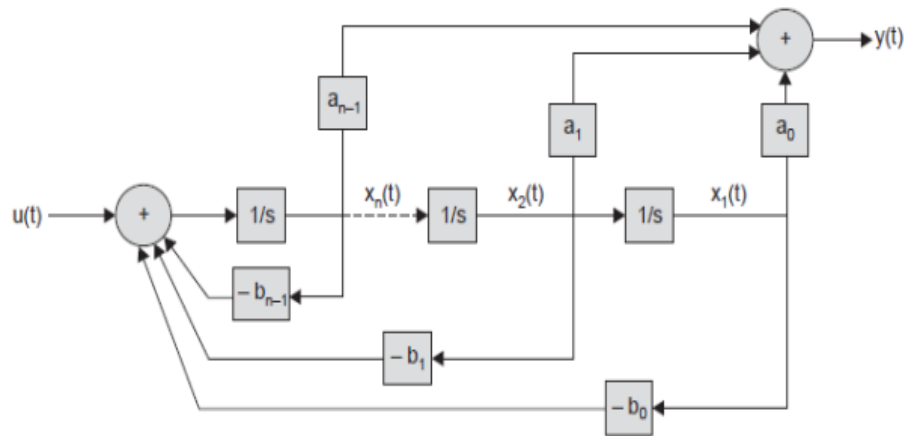


FIGURE 3.7: Simulation Diagram in State Variable Representation (Author).

form is depicted in Figure 3.8. The equivalence of the system in Figure 3.7 to the equation (3.33) can be established by calculating the transfer function $Y(s)/U(s)$ from the figure.

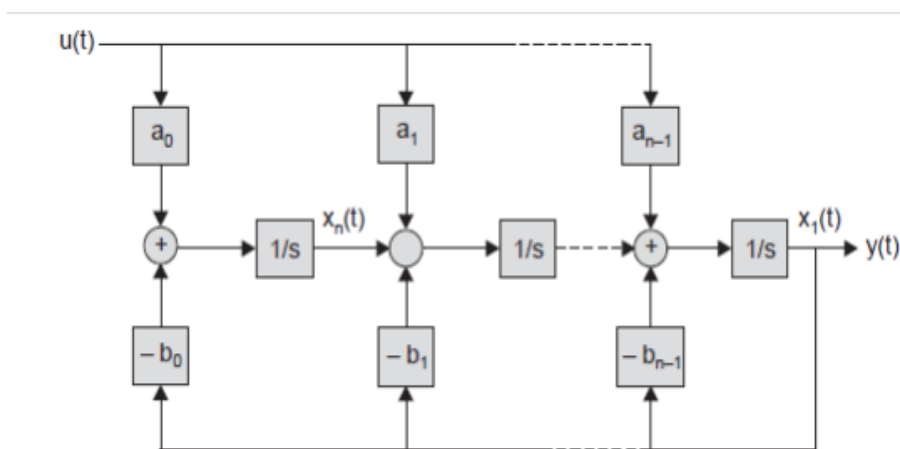


FIGURE 3.8: Observer canonical form (Author).

3.3 Parameter Identification for MGA Model

The convenient way of characterizing a DC Motor-Gear-Alternator is to carry out a separate test for each parameter. It is a time consuming process and can yield misleading output if the parameters are determined under no load or static conditions. A novel approach is necessary to obtain accurate parameters for better control. There are different methods studied and these are Pasek's, frequency response, pseudo-inverse, non-linear least square and pattern search methods (Salah, 2015).

3.3.1 Pasek's Method

Pasek's method is an earliest approach utilized for parameter identification of DC motor. It defines a high-performance model type and almost all the model parameters founded only on the current response of a system to a step input of armature voltage together with the steady state speed. However, the method can present some instrumentation problems. The method requires an accurate interpretation of two points of a transient waveform, which may be difficult to undertake in presence of noise. Besides, this approach determines a few points on the current time response-curve making it highly sensitive to current commutation noise, thus, rendering the method wildly inaccurate for the low-cost models that are widely employed in industries.

3.3.2 Frequency Response Method

An alternative approach to Pasek's method is through the frequency response approach for determining the systemic parameters of high performance. This

method has the following features:

- (i) All important system parameters are determined at once in a dynamic and loaded condition.
- (ii) No nonelectrical measurements are required (such as speed in Pasek's method).
- (iii) The output is averaged out in order to minimize errors produced by noise.
- (iv) Sophisticated instrumentation is not necessary.
- (v) The method is easily adaptable to automatic analysis.

The frequency response approach measures the parameters, in the model, of high performance by considering a second order model as the electrical impedance. By tuning the values of the circuit components to suit the response of the model and by some co-relations the parameters of the system are calculated. The approach uses an AC signal with precise frequency about 1kHz. However, this method is not appropriate to the power drivers employed in the model. The sensitivity to the noise is one of the reasons that discourage one to utilize this method.

3.3.3 The Pseudo Inverse Method

The pseudo inverse method is a method capable of identifying an equivalent discrete transfer function of simple systems like the thermal system, mass damper systems among others with no zeros (only poles). Although this approach assumes a single input single output system, it could not be used to find the DC Motor-Gear-Alternator parameters and doesn't fit the study's objective.

3.3.4 Step Response Method

Step response method is an overall approach for the identification of parameters that seeks to define the objective function that might reach its minimum (Hopgood, 2011). The physical model was described in terms of the parameters and the objective function was minimized with respect to the identified parameters by an iterative process. The author used Nonlinear Least Square, Pattern Search, Gradient Descent and Simplex Search algorithms.

3.3.5 Procedure for Parameters Identification

Parameter estimation used is the one outlined in (Salah, 2015). This method is built in Simulink Parameter Estimation software in MATLAB for the parameters identification of the MGA model. The Simulink Parameter Estimation algorithm was used for calibrating and estimating the system parameters from anticipated data. The algorithm supports the following types of estimation:

- (i) The transient estimation: It estimates the parameters through the comparison of model output to the anticipated data for a given input.
- (ii) Initial condition estimation: It estimates the preliminary conditions of states by utilizing expected data.
- (iii) The adaptive lookup tables: It estimates the table values at the set break-points by utilizing measurements from the physical model.

The Simulink Parameter Estimation algorithm provides the tools utilized to:

- (i) Set up the problem.

- (ii) Specify which model parameters to estimate.
- (iii) Import and prepare the expected data for parameter estimation (or pre-process).
- (iv) View the estimation progress.
- (v) Validate the estimation results based on plots of measured versus simulated data.

3.3.6 How Simulink Parameter Estimation Software Works

The Simulink Parameter Estimation algorithm compares empirical data with the output generated by the Simulink model. By employing the optimization techniques, the software approximates the parameter and the initial conditions of states in a way that the user-selected cost function is reduced. The cost function characteristically calculates the least-square error between the model and the empirical data signals. After the construction of a Simulink model, the following are used to configure and run parameter estimation:

- (i) Parameter Estimation in the Simulink model window is selected. It opens the Control and Estimation Tools Manager which creates a new project and adds an estimation node to the workspace directory tree.
- (ii) Import the input and output data set for estimating parameters of the Simulink model.
- (iii) Select the parameters and initial conditions you want to estimate.
- (iv) Configure the estimation, cost functions and data views.

- (v) Run the estimation.
- (vi) Check the results by examining the cost function values, plots, or parameter values.

3.4 Analysis of the MGA Model

Once an appropriate mathematical model of a system have been obtained, in transfer function form, the model is then analyzed to predict how the system will respond in both the time and frequency domains by using available mathematical tools. Transient Characteristics of Second Order Systems that store energy cannot respond instantaneously, so they exhibit a transient response when they are subjected to perturbed inputs or disturbances. Consequently, the transient response characteristics constitute one of the most important factors in system design (Gardner, 1942).

In various practical cases, the preferred performance features of control systems can be expressed in terms of transient response conditions and step inputs are usually employed input for this objective, since such an input is quite easy to generate. Mathematically, if the response of a given linear system to the step input is identified, by the principle of superposition and the assumptions of the linear theory, it is conceivable to calculate the systems response to any given input. However, the transient response of a given system to a unit step input is determined by the initial conditions.

For convenience of comparison between the transient responses of different systems, it is hence a common practice to employ the standard initial conditions; the model is initially regarded to be at resting state, with its output and general

derivatives set at zero to enable the comparison of various transient responses. Through the observation of these protocols, it will then be likely to compare the transient responses for different controller parameters and develop a design for the controllers depending on given transient response specifications. In broad terms, the transfer function of a second order system with input, $u(t)$ and the output, $y(t)$ (Golnaraghi & Kuo, 2010) can be expressed as,

$$G(s) = \frac{Y(s)}{U(s)} = \frac{k\omega_n^2}{s^2 + 2\zeta\omega_n s + \omega_n^2}, \quad (3.48)$$

Whereby, $U(s)$ and $Y(s)$ are the Laplace transforms associated with the $u(t)$ and $y(t)$ respectively, ζ is the damping ratio and ω_n is the resonant frequency. A system can be:

(i) Over damped ($\zeta > 1$)

The system returns (exponentially decays) to equilibrium without oscillating.

(ii) Critically damped ($\zeta = 1$)

The system assumes to equilibrium as quickly as possible without oscillating.

(iii) Under damped ($\zeta < 1$)

The system oscillates (at reduced frequency compared to the undamped case) with the amplitude gradually decreasing to zero.

(iv) Undamped ($\zeta = 0$)

The model oscillates at its natural resonant frequency (ω_0) without undergoing decay of its amplitude.

Figure 3.9 shows the effect of varying damping ratio on a 2nd order system.

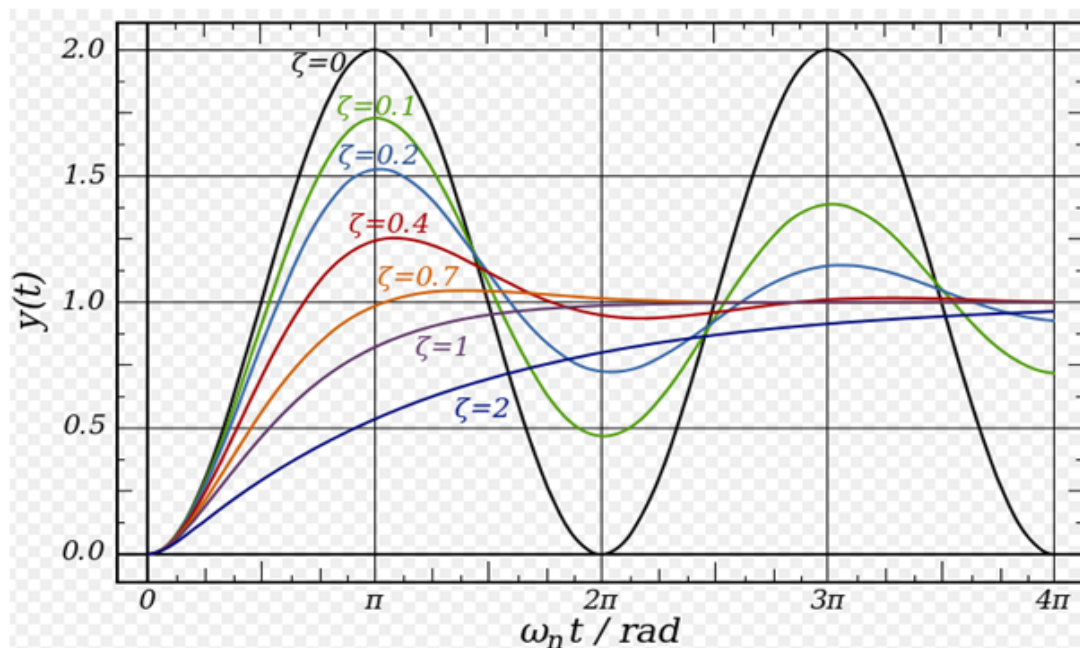


FIGURE 3.9: The Effect of Varying Damping Ratio on a 2nd Order System (Alciatore, 2007).

The response for such a given system is given in Figure 3.10 associated with the transient response stipulations that are well-defined below and any or all of the subsequent parameters can be used to postulate such responses completely. Figure 3.10 demonstrates a typical unit-step response of a recilinear analog control model. With respect to the unit-step response, the performance criteria usually used for the description of linear control models in the time domain are defined as follows:

(i) Rise time (t_r): The time needed for the signal to change from a given low

value to a specified high value. Characteristically, these values are 10% and 90 % of the input step size.

- (ii) Maximum Overshoot (Mp): It is the maximum peak value of the specific response curve determined from the step input of the system.
- (iii) Percentage Overshoot (PO) is the difference between the peak value and the input step size , as a percentage of the step size.
- (iv) Settling time (t_s): This is the time passed from the application of the ideal instantaneous step input to the period at which the output has achieved and persisted within the specified error band (notably within the 2 % or 5 % within the final value).
- (v) The delay time (t_d): Time needed for the response to attain half the final value the initial time.
- (vi) Peak time (t_p): The time needed for the response to achieve the first peak of the over-shoot.
- (vi) The steady-state error (e_{ss}): The difference between the preferred final output y_{des}^{ss} and the real response when the model reaches a steady state (y_{ss}), as soon as its behavior may be probable to continue if the system is uninterrupted.

In most actual applications, desired values of these parameters would be provided and the objective would be to design the controllers that can merge the requirements. Some required characteristics in addition for a dynamic system to be steady, that is, its response does not increase with time (a requirement that was

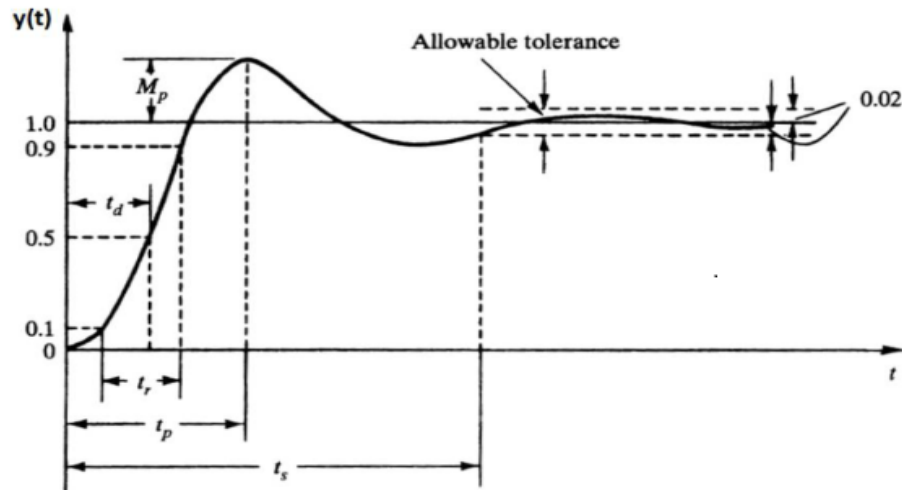


FIGURE 3.10: Typical 2^{nd} Order Step Response (Vaishnav and Khan, 2007).

satisfied for the second order model provided that $\zeta \geq 0$) and the system should hold the following;

- (i) The instantaneous and faster response
- (ii) Minimal over-shoot should be beyond the desired value (relatively stable)
- (iii) Ability to reach and remain averagely close to the preferred reference value in the minimum time possible.

The investigator utilized these parameters to analyze the MGA system under various forms of controls and maximize the controller gains to obtain desired performance.

In some procedures, it is preferable to have high over-shoot and return quickly to the steady state. However, the high over-shoot is a problem in various processes. For instance, overshoot is not allowable in plastic glove manufacturing processes to prevent plastic film wrinkle (J. Basilio & Matos, 2002). Several tuning approaches

TABLE 3.1: *System Specification*

Parameter	Symbols (units)	Formula
Rise time	$t_r(s)$	$\frac{\pi - \beta}{\omega_d}, \text{ where}$ $\beta = \tan^{-1} \left[\frac{\sqrt{1 - \zeta^2}}{\zeta} \right]$ $\omega_d = \omega \sqrt{1 - \zeta^2}$
Maximum overshoot	$M_p(\%)$	$\frac{-\zeta\pi}{e^{\sqrt{1-\zeta^2}} \times 100}$
Delay time	$t_d(s)$	$\frac{1 + 0.7\zeta}{\omega_n}$
Settling time	$t_s(s)$	$\frac{4}{\zeta\omega_n} \text{ (2 \% settling time)}$ $\frac{3}{\zeta\omega_n} \text{ (5 \% settling time)}$
Peak time	$t_p(s)$	$\frac{\pi}{\omega_d}$
Steady state error	e_{ss}	$\lim_{t \rightarrow \infty} y(t) - y_{des}^{ss}$

focused on controller parameter modification in order to lower the excessive overshoot to the specific overshoot of a closed-loop system. (J. Basilio & Matos, 2002) proposed a tuning law for a systematic adjustment of the controller gain to produce a closed loop response without overshoot. (Skogestad, 2003) suggested the Direct Synthesis (DS) approach equivalent to a time delay in order to create a response with 5% overshoot. Abbas (1997) developed controller tuning co-relations associating the overshoot and model parameters through the modification of the DS tuning method. The design must possess the following specifications (Zhang & Messner, 2011)

- (i) Maximum overshoot must be less than 20 %.

- (ii) The steady-state error should be less than 3 %.

- (iii) Settling time should be less than 5 seconds.

- (iv) The peak value should be less than 3 units.

3.5 Stability of the MGA Model

In this section, the techniques such as Routh-Hurwitz criterion, Nyquist Diagram plots and Bode plots are utilized to test the stability margin of the MGA model.

3.5.1 The Routh-Hurwitz Method

It is a useful method for assessing the nature of the roots of a characteristic equation without solving it explicitly. The technique allowed the investigator to compute the number of roots of the typical equation that was located on the right-hand plane of the imaginary axis of the s -plane. It can be exploited as a designing tool for determining the data of some system parameters to guarantee the stability of the closed loop models. Once the stability was assured, the question of relative stability can be taken up to find the level of stability of the closed loop systems. Edward John Routh and Adolf Hurwitz independently published in the 1890s, a method of investigating the stability of a linear system (Hurwitz, 1964). The Routh-Hurwitz stability strategy offers an excellent response to the question of

stability by examining the characteristic equation of the model. The characteristic equation in the s -domain was written as;

$$Q(s) = a_0s^n + a_1s^{n-1} + \dots + a_{n-1}s + a_n = 0. \quad (3.49)$$

Equation (3.49) is written in factored form to determine if some of the roots of $Q(s)$ lie in the right half of the s -plane or not, hence

$$a_0(s - \alpha_1)(s - \alpha_2)\dots(s - \alpha_n) = 0, \quad (3.50)$$

where $\alpha_i = i^{th}$ are root of the characteristic equation.

From relation (3.50), the following two fundamental conditions were obtained;

- (i.) All the coefficients in the above polynomial are of the same sign and are nonzero
- (ii.) None of the roots possess positive real parts.

These conditions are essential but not sufficient that means that, if these features are not satisfied; it could immediately be concluded that the model was unstable; however, even if these conditions were met, the stability is not guaranteed.

The Routh-Hurwitz criterion was both sufficient and necessary condition for ensuring the stability of linear systems. The strategy was originally presented in terms of the determinants generated with the components of characteristic equation using the array formulation in a tabular form which is more convenient. The

characteristic equation of an n^{th} order system was considered as,

$$\alpha_0 s^n + \alpha_1 s^{n-1} + \alpha_2 s^{n-2} + \dots + \alpha_{n-1} s + \alpha_n = 0. \quad (3.51)$$

The Routh-Hurwitz criterion of stability analysis was stated in terms of the coefficients of the given characteristic equation organized in a tabular presentation as shown in Table 3.2. .

TABLE 3.2: *Routh-Hurwitz Criterion*

s^n	a_0	a_2	a_4	$a_6 \dots$
s^{n-1}	a_1	a_3	a_5	$a_7 \dots$
s^{n-2}	b_1	b_2	b_3	$b_4 \dots$
s^{n-3}	c_1	c_2	c_3	$c_4 \dots$
s^{n-4}	d_1	d_2	d_3	$d_4 \dots$
\vdots	\vdots	\vdots	\vdots	\vdots
s^2	e_1	e_2	0	$0 \dots$
s^1	f_1	0	0	$0 \dots$
s^0	g_1	0	0	$0 \dots$

The first row in the table above is formed by writing the alternative coefficients of the characteristic equations starting with the coefficients of the highest power s^n . Similarly, the second row is composed of writing the alternative coefficients of the characteristic equation starting with the coefficient of s^{n-1} . The coefficients b_1, b_2, b_3, \dots , are evaluated, in terms of the elements from the first two rows, as indicated in equations (3.52),(3.53) and (3.54).

$$b_1 = \frac{(a_1a_2 - a_0a_3)}{a_1} \quad (3.52)$$

$$b_2 = \frac{(a_1b_4 - a_0a_5)}{a_1} \quad (3.53)$$

$$b_3 = \frac{(a_1a_6 - a_0a_7)}{a_1} \quad (3.54)$$

and so on.

The calculation of the components in the third row was continued till all components became zero. A similar procedure is followed in assessing the entries denoted by c 's, d 's, e 's, and so on with regards of the components of the previous two rows.

That is,

$$c_1 = (b_1a_3 - a_1b_2)/b_1 \quad (3.55)$$

$$c_2 = (b_1a_5 - a_1b_3)/b_1 \quad (3.56)$$

$$c_3 = (b_1a_7 - a_1b_4)/b_1 \quad (3.57)$$

$$d_1 = (c_1b_2 - b_1c_2)/c_1 \quad (3.58)$$

$$d_2 = (c_1b_3 - b_1c_3)/c_1 \quad (3.59)$$

$$d_3 = (c_1b_4 - b_1c_4)/c_1 \quad (3.60)$$

Quadratic Polynomial

Consider the quadratic polynomial:

$$a_0s^2 + a_1s + a_2 = 0, \quad (3.61)$$

where all the a_i ; $i = 0, 1, 2$ are positive .The array of coefficients becomes;

TABLE 3.3: *Array of Coefficients*

s^2	a_0	a_2
s^1	a_1	0
s^0	a_2	

The coefficient a_2 is the result of,

$$a_2 = (a_1 a_2 - a_0(0))/a_1 \quad (3.62)$$

In the case of a second order polynomial, it was observed that Rouths stability criterion reduces to the condition that all a_i be positive.

3.5.2 Nyquist Method

The Nyquist criterion is described as a graphical approach, which allows for the determination of the stability of a given closed-loop model from the open-loop transfer function.

The Nyquist approach has the following characteristics that make it approximate for the analysis and design of the MGA model:

- (i) It offers the same information on the ideal stability of a given control system as does the Routh-Hurwitz approach.
- (ii) In addition to absolute model stability, the Nyquist strategy provides data for the relative instability or stability of a system.

- (iii) Provides feedback about improving the stability, as deemed necessary.
- (iv) The frequency- domain plots of loop gain $G(j\omega)H(j\omega)$ give information on the frequency domain features of the closed-loop model.

For the SISO (Single-Input Single-Output) feedback system the closed-loop transfer function is given by Figure 3.11

The closed-loop transfer function is

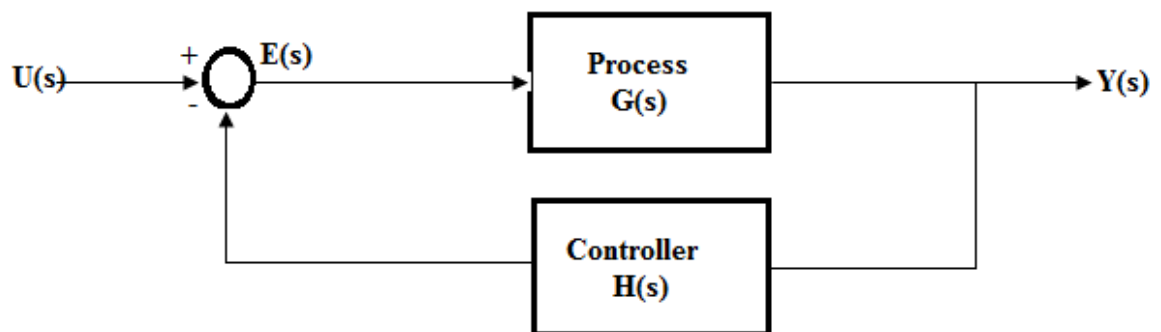


FIGURE 3.11: Single Loop Feedback Control System (Author).

$$M(s) = \frac{G(s)}{1 + G(s)H(s)}, \quad (3.63)$$

whereby, $G(s)$ denotes the system and $H(s)$ represents the feedback component and $E(s)$ is the design variable. Since the model poles are measured as those values that its transfer function turns to infinity, it follows that the closed-loop model poles are obtained by working out the following equation

$$1 + G(s)H(s) = 0 \quad (3.64)$$

Which represents the system characteristic equation. The following complex function was obtained

$$D(s) = 1 + G(s)H(s) \quad (3.65)$$

whose roots are characteristic of the closed-loop poles of the transfer equation. In addition, it can be seen that the roots of $D(s)$ represent the poles of $M(s)$. The roots of $D(s)$ are the open-loop control model poles since they are influenced by the roots of $H(s)G(s)$ that can be regarded as the open-loop control model transfer function achieved when the feedback loop is open at some point. All of the roots $D(s)$ must lie in the left-hand s -plane for stability. A contour Γ_s was chosen, in the s -plane which encloses the entire right-hand s -plane and plot Γ_D in the $D(s)$ -plane and determine the number encirclements of the origin. Equivalently, the Γ_p could be plotted in the $p(s)$ -plane and determine the number of encirclements of -1 point, where $p(s)=D(s)-1$. The stability criterion can be stated as in section 3.7.5. The Nyquist stability measurement is achieved by applying the Cauchy principle of argument to the complex function $D(s)$.

Let $F(s)$ represent analytic equation in a closed part of the complex plane given in Figure 3.12 except at a finite number of points (namely, the poles of $F(s)$). It is assumed that it is analytical at every region on the contour. Then, as s travels through the contour in the s -plane towards the clockwise direction, the equation $F(s)$ encircles the origin in the $F(s)$ - plane in the same direction N times and is given by;

$$N = Z - P, \quad (3.66)$$

whereby, P and Z represent the number of poles and zeros of the equation $F(s)$ inside the contour, respectively. The Nyquist plot is the polar plot of the function

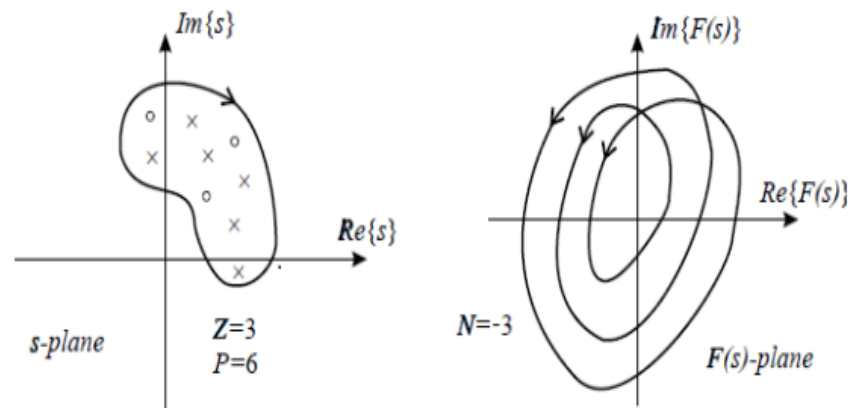


FIGURE 3.12: Cauchy's Principle of Argument (Author).

$D(s)=1+G(s)H(s)$ when s travels around the contour given in Figure 3.13. The

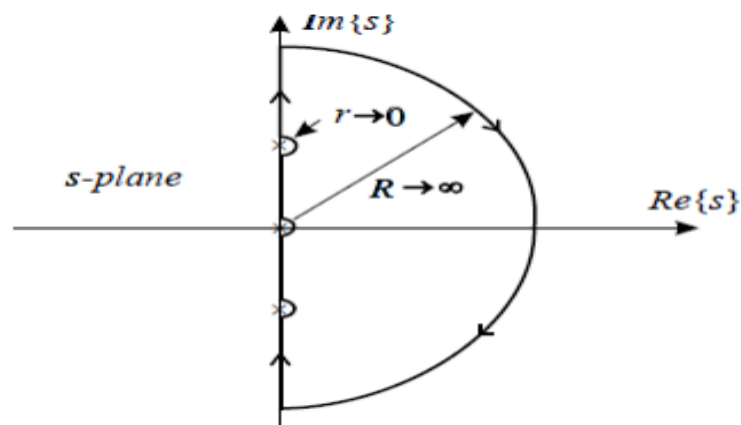


FIGURE 3.13: Contour in the S-Plane (Author).

contour covers the unstable half-plane of the complex plane $s \rightarrow \infty$. Given the function $D(s)$, according to the Cauchy's principle of argument, should be analytic at each point on the contour, the poles of the $D(s)$ in the imaginary axis must be encircled by insignificant small semicircles. The Nyquist plot is determined by plotting a locus of imaginary ($G(j\omega)$) versus Real($G(j\omega)$) at the full range of frequencies $(-\infty, \infty)$. It is easier to obtain Nyquist plots by hand or by using some software packages such as Matlab (Dorf & Bishop, 2011).

Nyquist Stability Criterion states that, a feedback control system of equation (3.63) is stable if and only if, for the contours Γ_p , the number of counterclockwise encirclements of the (-1,0) point is equal to the number of poles of $p(s)$ with positive real parts.

Two vital notions can be obtained from the Nyquist diagram; the gain and phase stability margins. The gain and phase stability margins give the degree of relative stability; in other words, they tell how far the given system is from the instability region.

Nyquist open loop polar plot indicates the degree of stability, the adjustments required and provide stability information for systems containing time delays. Polar plots are not used in this work because, without powerful computing facilities, they can be difficult to generate at a detailed level and they do not directly yield frequency values (Lisle, 1997).

3.6 Suitable Range of the Gear Ratio for the MGA Model

From the Bode Plot

The complex equation $G(j\omega)H(j\omega)$ might be shown by two separate graphs (Mandal, 2006), one giving the magnitude against frequency and the phase angle (in degrees) versus the frequency as shown in Figure 3.14. The logarithm of the magnitude $G(j\omega)H(j\omega)$ was used in the Bode diagram and the frequency was also plotted in the logarithmic scale, both for the amplitude and the phase angle. The universal representation of the logarithmic magnitude of the $G(j\omega)H(j\omega)$ function was $20 \log[G(j\omega)H(j\omega)]$, whereby, the base of the logarithm was 10. The critical advantage of using logarithmic plot for the frequency response of transfer function

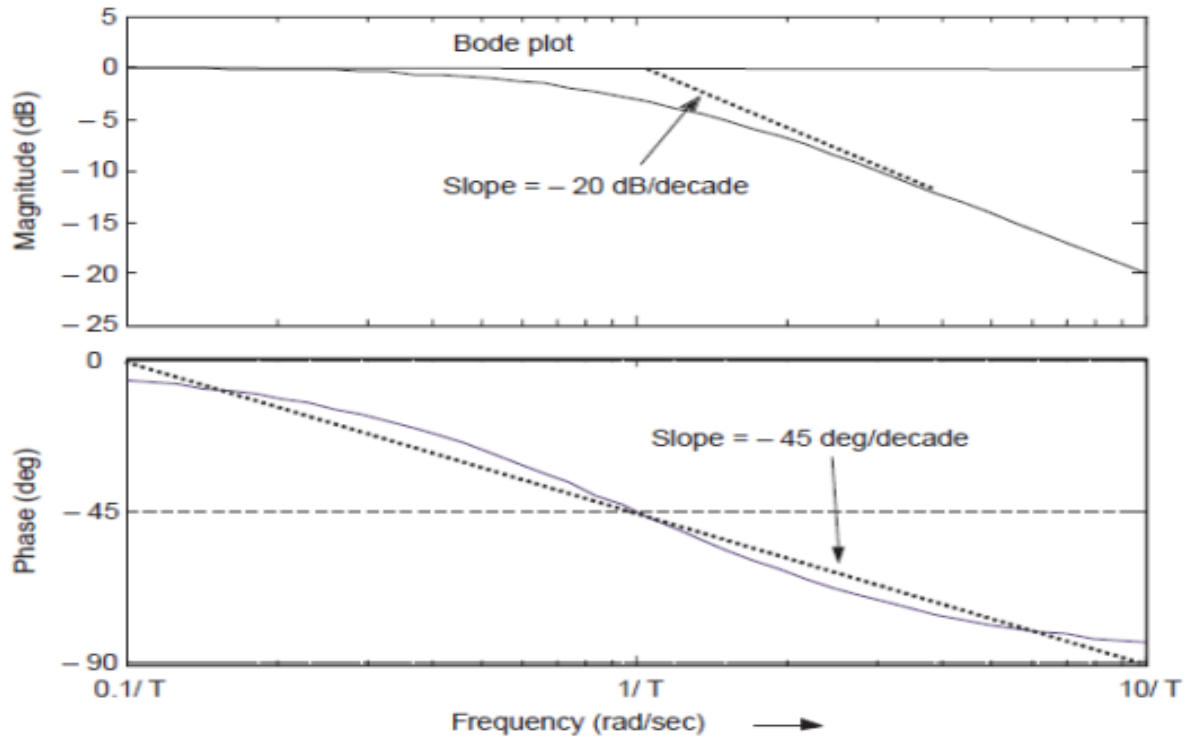


FIGURE 3.14: Bode Plot of Simple Pole (Mandal, 2006).

was that it permits a simpler method for achieving the approximate log-magnitude curve of the transfer equation. It is based on straight-line asymptotic estimations, which is adequate for the rough sketching of the frequency response properties required in the design stage.

The utilization of logarithmic scale enables to display both in the low-frequency and high-frequency of the transfer function in a single graph. Even though the zero frequency cannot be involved in the logarithmic scale, it is not a critical problem as one can assume a low frequency since it is required for the analysis and the design of practical control system.

Bode plots are extensively used in the preliminary stages of analysis and design of a control system, since they give the general nature of the frequency-response characteristics quickly and fairly accurately with a minimum amount of calculation. After the design is complete, the detailed simulation of the entire system is

undertaken for final implementation.

Chapter 4

Simulation, Testing, Discussion and Results

4.1 Introduction

In this chapter, the researcher presented and discussed the findings using the Methods and Tools discussed in Chapter 3. The data were estimated and then processed in response to the objectives posed in chapter one of this thesis. The results of the data have been analyzed using the MATLAB software to identify, describe and explore the stability of the MGA model to determine the applicability of the system.

4.2 Description of the DC Motor-Gear-Alternator Simulink Model.

The model of the DC Motor-Gear-Alternator was designed using Simulink as discussed in chapter 3. The model consists of input port for acquiring input signal of motor voltage and the output port for acquiring the output signals of alternator

voltage. The Simulink Block diagram used for simulation is shown in figure 4.1.

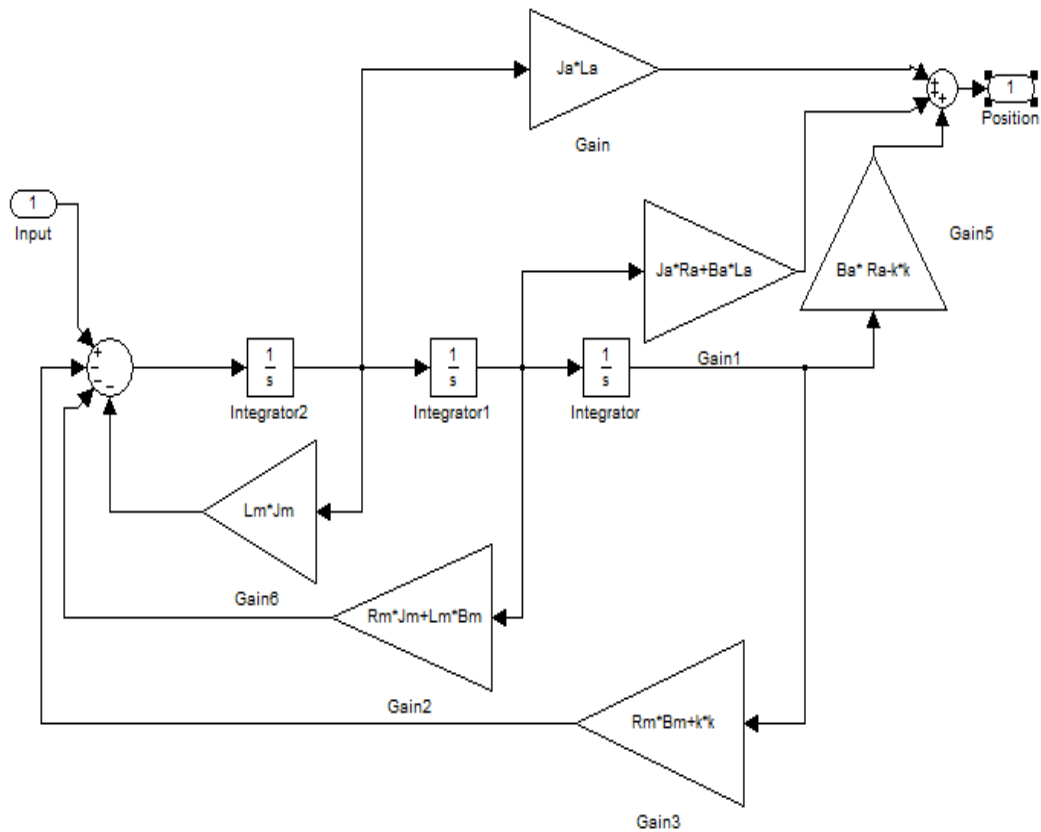


FIGURE 4.1: Block Diagram of DC Motor-Gear- Alternator System. (Koech et al., 2016).

4.3 System Parameters

The designing parameters are the, B_a Viscous friction coefficients of the alternator, B_m Viscous friction coefficients of the motor, J_a Moment of inertial of alternator, J_m Moment of inertial of motor, K Torque Constant of the system, L_a Inductance of the alternator, L_m Inductance of the motor, R_a Armature Resistance of alternator, R_m Armature Resistance of the Motor. Before running the model, the numerical values were assigned to each of the variables used in the model .For convenience of comparison between the transient responses of different systems, it is a common practice to employ the standard initial conditions. The model is initially regarded to be at resting state and therefore, for the MGA system, the

initial values of each parameter were set at zero or $[0,0,0,0,0,0,0,0]$.

Figure 4.2 shows the voltage response of the model using the initial parameter values in the model with a unit input voltage. Figure 3.10 shows the required step response. Obviously the parameters had to be estimated so that the system could respond as required. The Simulink Parameter Estimation tool supports the optimization of the problem.

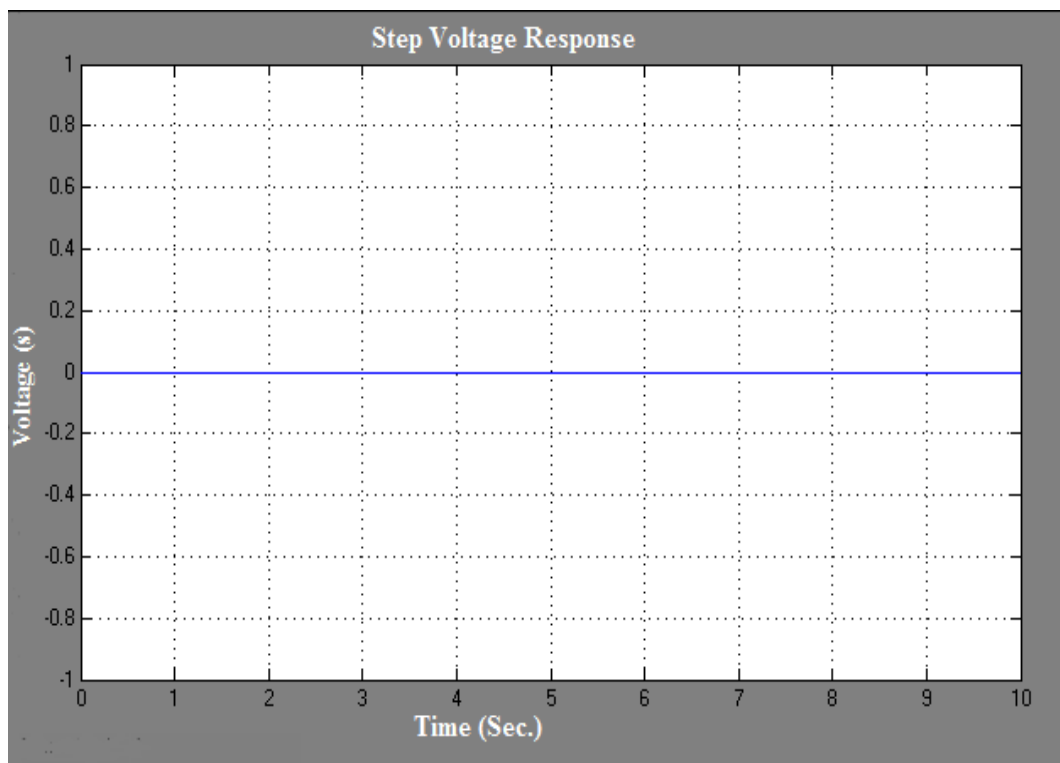


FIGURE 4.2: Voltage Response of the Model Using the Initial Parameter Values.

4.3.1 Data Estimation

A new data set could be generated by clicking on the **Transient Data** button and followed by clicking on the **New** button in the right-hand-side of the window. The data sets could then be utilized for estimation and or validation. Three data sets were identified; the first one was employed for parameter estimation and the other two for validating the characteristic response of the Simulink tool with the

estimated parameters. The data sets could be imported from different sources involving the MATLAB variables, Excel files, MAT files, or comma-separated-value files. After importation of data, a plot was generated to confirm that the right data sets in the estimation project were selected. A new data set could be generated by clicking on the **Transient** data button and followed by clicking on the **New** button in the right-hand-side of the window. The data sets could then be utilized for estimation and or validation.

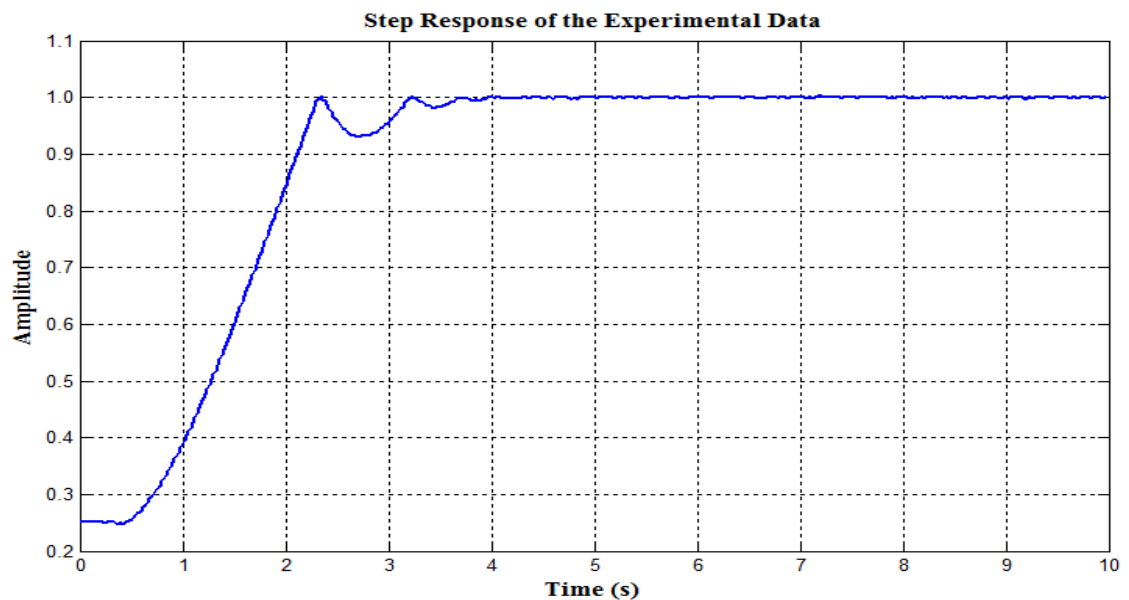


FIGURE 4.3: Expected Response of the MGA.

Figure 4.3 shows the expected response of the model and Figure 4.2 shows the voltage response from MGA model. It was found that MGA initial data did not match the measured data since the parameters are not correct. Hence, the Simulink optimization tool was utilized to automatically adjust the MGA model parameters.

4.3.2 Definition of Variables to be Estimated

This step involved the definition of variables for the estimation process. The simulation parameters could be adjusted, together with the rules that govern the values. The Estimation variables are chosen by clicking on the **Variables** button and pressing on the **Add** button. It opens a **Parameter** Selection Dialog from which the model parameters are selected for estimation.

At this point nine unknown parameters had been added to the model using the

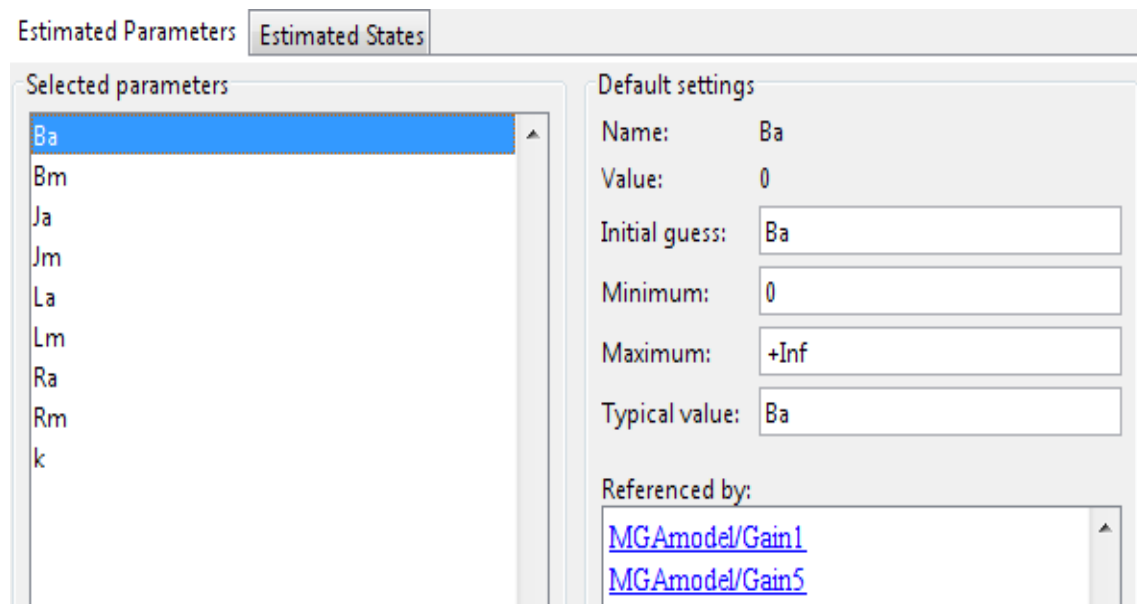


FIGURE 4.4: Selecting Parameters for Estimation.

selection dialog. The parameters are the B_a , B_m , J_a , J_m , L_a , L_m , R_m , R_a and K . On the right-hand side of the window, the initial predictions for the parameter values are set, as well as the minimum and the maximum bounds as shown in Figure 4.5. The physical insight demonstrated that all of the parameters have positive values. Hence lower limits and initial value for the parameters were set to zero.

4.3.3 The Estimation Task of Parameters

In order to run estimation, the **Estimation** node should first be created. This is done by clicking on the **Estimation node** and pressing the **New** button in the right-hand-side panel. In the project, an estimation node called **New Estimation** was created. The first panel is where the data sets to be used in this estimation were adjusted. It was possible to employ one or more data sets at a go in a given estimation. The data set called **Estimation Data** were used to predict the data set. The next panel called **Parameters** is where the investigator selected the parameters to adjust in this estimation. Even though the researcher selected nine parameters, in general, it was necessary to estimate all of them at once since the model was simple enough to estimate all the nine parameters.

Name	Value	Estimate	Initial Guess	Minimum	Maximum	Typical Va...
Ba	0	<input checked="" type="checkbox"/>	Ba	0	+Inf	Ba
Bm	0	<input checked="" type="checkbox"/>	Bm	0	+Inf	Bm
Ja	0	<input checked="" type="checkbox"/>	Ja	0	+Inf	Ja
Jm	0	<input checked="" type="checkbox"/>	Jm	0	+Inf	Jm
La	0	<input checked="" type="checkbox"/>	La	0	+Inf	La
Lm	0	<input checked="" type="checkbox"/>	Lm	0	+Inf	Lm
Ra	0	<input checked="" type="checkbox"/>	Ra	0	+Inf	Ra
Rm	0	<input checked="" type="checkbox"/>	Rm	0	+Inf	Rm
k	0	<input checked="" type="checkbox"/>	k	0	+Inf	k

FIGURE 4.5: Selecting Which Parameters to Adjust in this Estimation.

4.3.4 Viewing the Results

Figure 4.6 below shows the initial Voltage response of the MGA system overlaid the expected response. As the parameters values improved, the simulation curves

get closer to the expected data.

Four plot types are created to view the estimation results. The plots in Figure

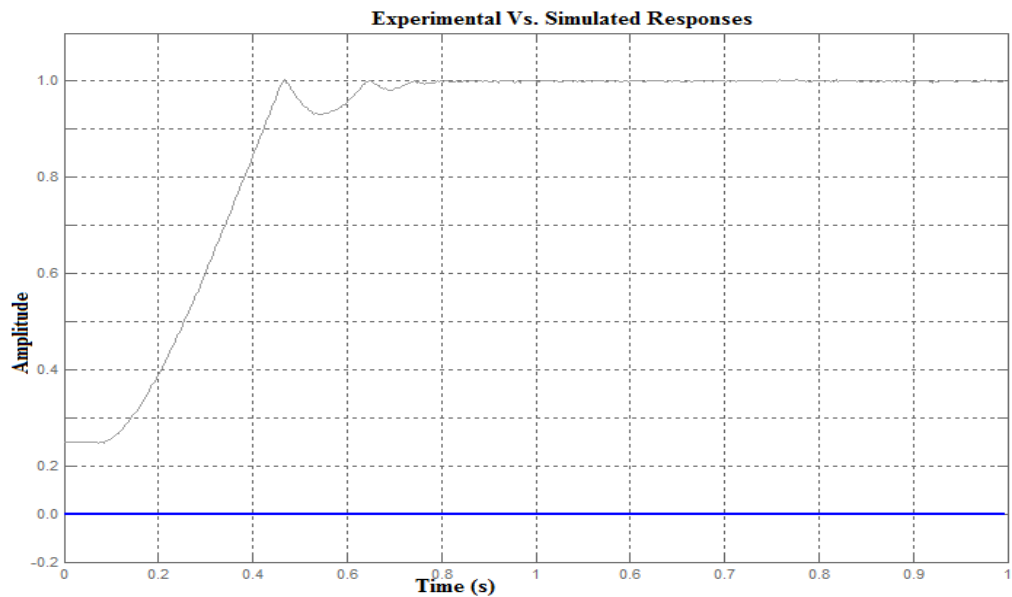


FIGURE 4.6: Initial Voltage Response for the Actual and Estimated Models.

4.7 shows the expected data fell within the expected range with the simulated data. The estimation outcome appeared satisfactory for nonlinear least square and Pattern search algorithms since the estimated (blue) and (red) curves relatively matched the measured results.

The plots in figure 4.8 shows the trajectory of the parameters at every estimation iteration stage. It was demonstrated that the parameters settled to the final values as the approximation process converges to a solution.

Table 4.1 showed the results for the four algorithms used. It can be seen that the values of the Nonlinear Least Square method and Pattern Search method are approximately the same with minimum error.

The transfer function of the DC Motor-Gear-Alternator model is needed for studying the state of the system and utilizing the controlling methods on it. The transfer function of the MGA model was derived by substituting parameter values

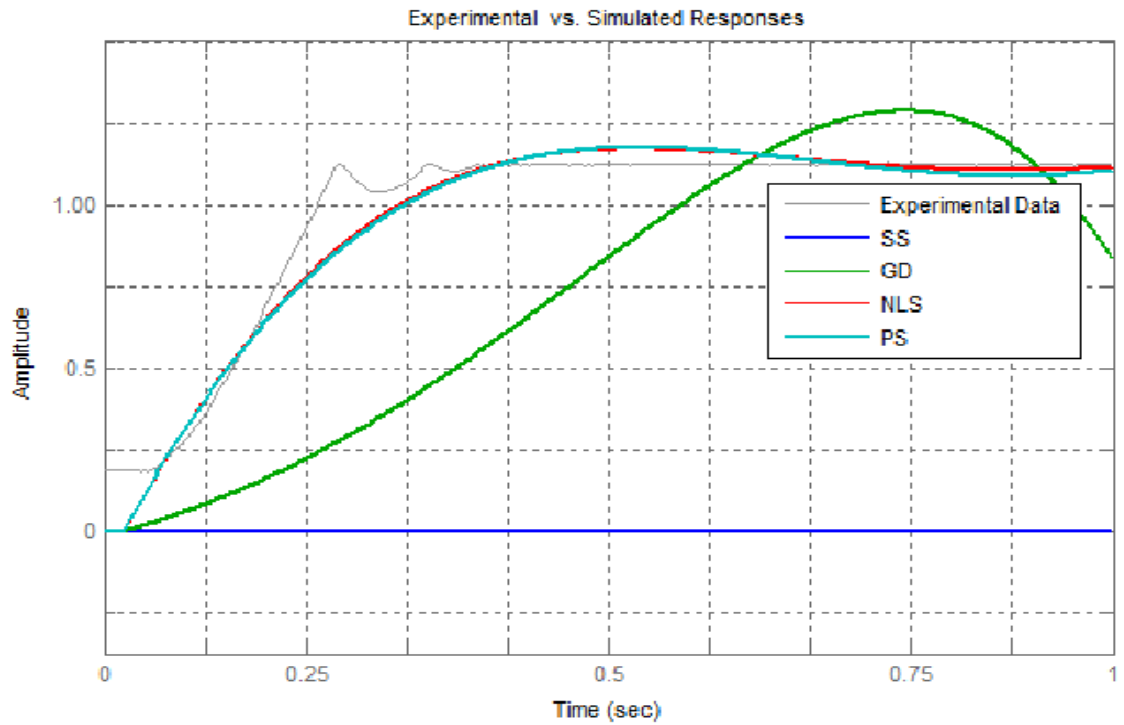


FIGURE 4.7: Voltage Response for the Experimental Data and Estimated Models.

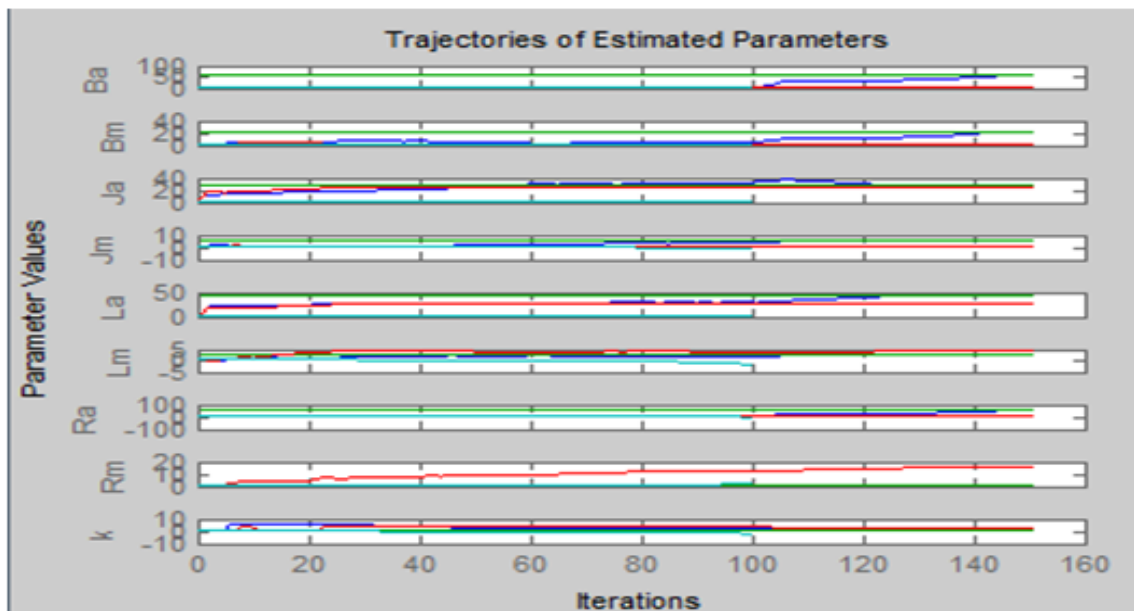


FIGURE 4.8: Trajectories for Parameters.

into equation (3.32) to obtain,

$$G(s) = G_r \left[\frac{-58.59s^2 - 9.82s - 0.14}{53.93s^2 + 25.23s + 2.94} \right] \quad (4.1)$$

TABLE 4.1: *Parameter Estimation Results*

Parameters	NLS	PS	GD	SS
B_a	0.8435	0.8436	1.9002	0.4711
B_m	1.5983	1.5983	0.0001	0.2521
J_a	7.1570	7.1560	26.1131	0.0191
J_m	9.3961	9.3960	0.9301	-0.0321
L_a	8.1859	8.1860	26.8013	3.9631
L_m	5.7396	5.7396	4.3030	-1.8440
R_a	0.4082	0.4081	1.5306	-0.1444
R_m	1.7084	1.7085	15.5302	2.2781
k	0.4553	0.4639	3.1012	-2.1442

Equation (4.1) is the transfer function of MGA model.

4.4 Analysis of MGA model

To calculate the damping ratio, ζ , the investigator used the equation (3.48) to compute as follows;

$$G(s) = G_r \left[\frac{1}{53.93s^2 + 25.23s + 2.94} \right] \quad (4.2)$$

where $\omega_n = 2.937$

$$\zeta = 25.23 / (2 * \sqrt{2.937}) = 7.36097 > 1$$

$$k = G_r / 2.937.$$

This shows that $\zeta > 1$ and hence the MGA system is overdamped. This means that the system returns (exponentially decays) to equilibrium without oscillating and do not exhibit oscillatory behavior when they are disturbed from their position of static equilibrium.

Figure 4.9 shows the open-loop step response The MGA gain of the plant transfer function was $77/200$, so 0.385 was the final value of the results to the unit step input. It reflects the steady-state error of 0.615 , quite large indeed. Furthermore,

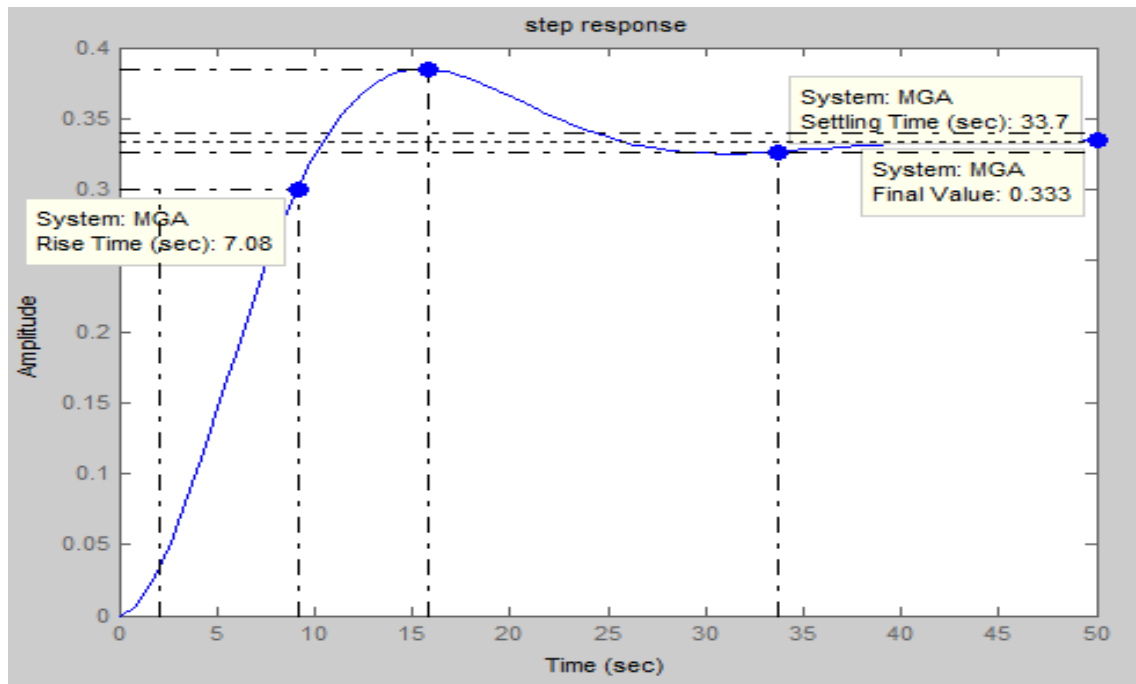


FIGURE 4.9: Response of the MGA Model.

the rise time is 7.08 seconds, and the settling time is about 33.7 seconds.

The next step is to design a controller that will reduce the rise time, reduce the settling time, and eliminate the steady-state error. Figure 4.9 shows the voltage response of the model using the initial parameter values in the model with a unit input voltage. Figure 3.10 shows the required step response. It is obvious that a tuning controller is required. It was compared that the impact of each of the PID determinants on the closed-loop dynamics and show how to utilize the PID controller to enhance the system performance. The PID controller works in a closed loop system using the schematic shown in figure 4.10. The variable (e) was the tracking error, the variability between the optimum input value (r) and the real output(y). The error signal (e) would be sent to the PID controller. Consequently, the controller calculate the derivative and the integral of the error signal. The control signal (u) to the plant is equal to the proportional gain (K_p) times the magnitude of the error plus the integral gain (K_i) multiplied by the the

integral of the error together with the derivative gain (K_d) times the derivative of the error.

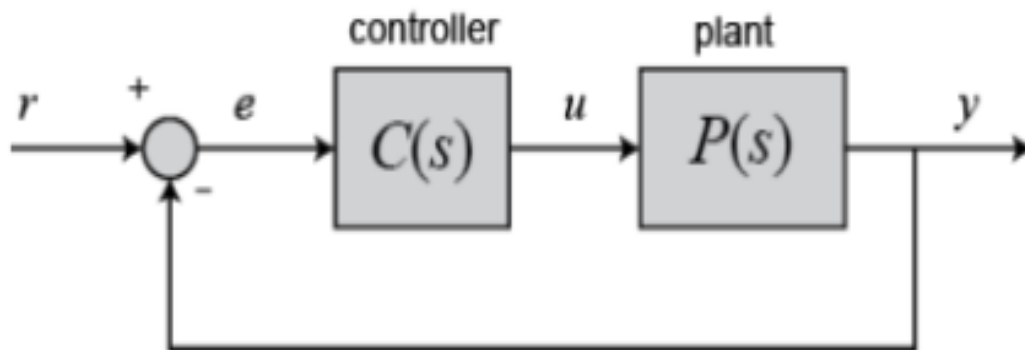


FIGURE 4.10: Unity Feedback System (Visioli, 2001).

The Simulink block with PID controller is shown in figure 4.11. When the Simulink

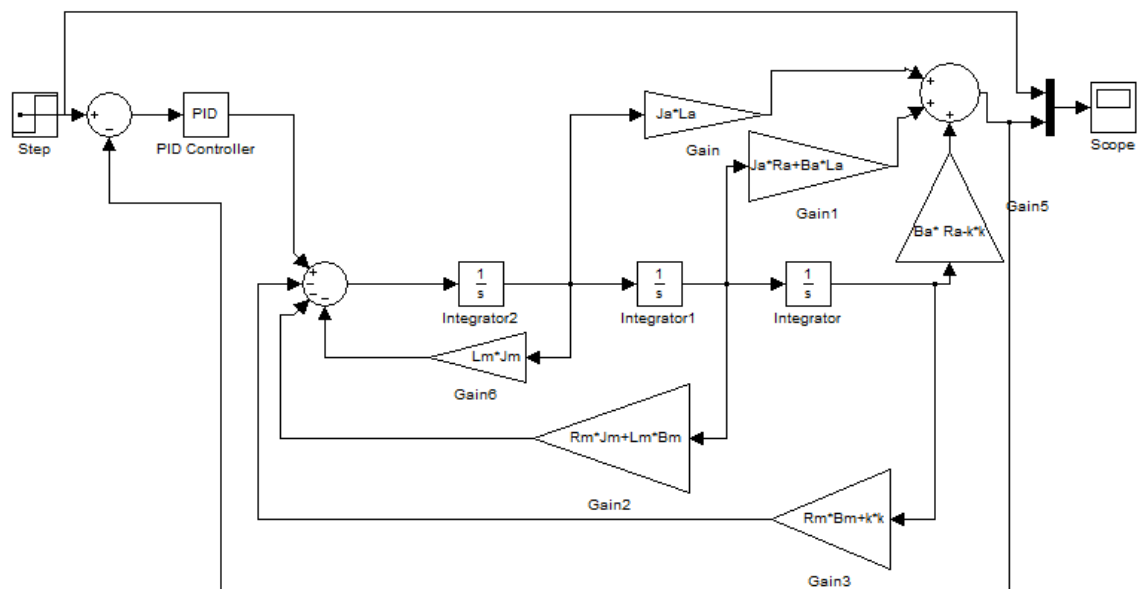


FIGURE 4.11: Simulink Block with PID Controllers.

of Figure 4.11 is run using initial parameter values, the output is shown in Figure 4.12a.

For this set up, K_p , K_i and K_d controllers having gains of 1000, 1000 and 350 respectively were used. Figure 4.12 b, c and d show the closed loop step voltage response of the actual and estimated model for the PID controllers. It can be observed that the proportional controller K_p reduces the rise time, the overshoot,

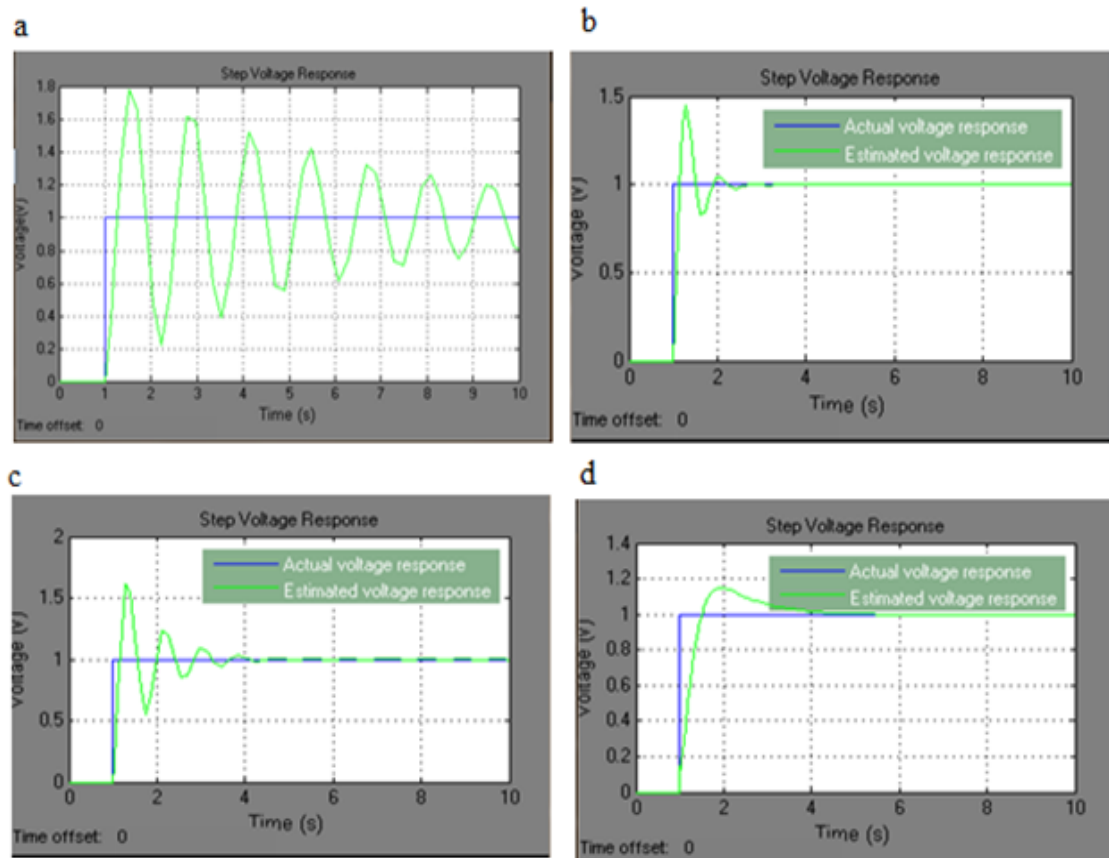


FIGURE 4.12: Step Response: (a) Response Without Controller (b) Response With Proportional Controller (c) Response With Integral Controller (d) Response With Derivative Controller.

and the steady-state error but minor change on the settling time. An integral controller K_i minimizes the rise time, elevate both the overshoot and the settling time, and eliminates the steady-state error, while the derivative controller K_d reduced the settling time, overshoot, and experienced a small effect on the increase of steady-state error and time. It is observed that PID controller rectify the overall performance of system and it improves transient as well as steady state response. The impacts of every of controller parameters, K_p , K_i and K_d on a closed-loop system are summarized in the Table 4.2.

TABLE 4.2: *Table of Different Values of PID Parameters*

Controller	Rise Time	Overshoot	Settling Time	S-S Error
k_p	Reduce	Lessen	Small Change	Decrease
k_i	Minimize	Increase	Increase	Eliminate
k_d	Slight Change	Lower	Decrease	Small Change

4.5 Open Loop Stability Analysis of The System

The characteristic equation observed on the transfer function (4.1) in the s-domain was given as $53.93S^2 + 25.23S + 2.93$. The criterion implies that for a system to be stable there should not be any changes in sign in the entries in the first column of the table (Stépán & Insperger, 2006). It is a both necessary and a vital condition for ensuring stability. When the roots of the polynomial equations were calculated, The results were obtained as follows

$$P = -0.2197$$

$$P = -0.2481$$

This shows that the system is stable since the real parts of the poles are both negative. The above polynomial was in agreement with the necessary condition for Routh's stability since all the coefficients are positive and nonzero. Writing the Routh array, the values were obtained as show in the Table 4.3

Given that the signs of the entries on the first column did not change the sign,

TABLE 4.3: *Routh's Table*

Column 1	column 2	column 3
s^2	53.93	2.94
s^1	25.23	0
s^0	2.94	

the system is stable.

4.6 Closed Loop Stability Analysis

The script used to generate the Nyquist plot for the system in Figure 4.13 is shown in the appendix A. According to the Nyquist criterion stated in Section 3.6.2, the number of poles of $G(s)H(s)$ characterized with positive real parts was zero and the total number of the counter-clockwise encirclements of -1 is zero. This shows that the closed-loop MGA system is stable.

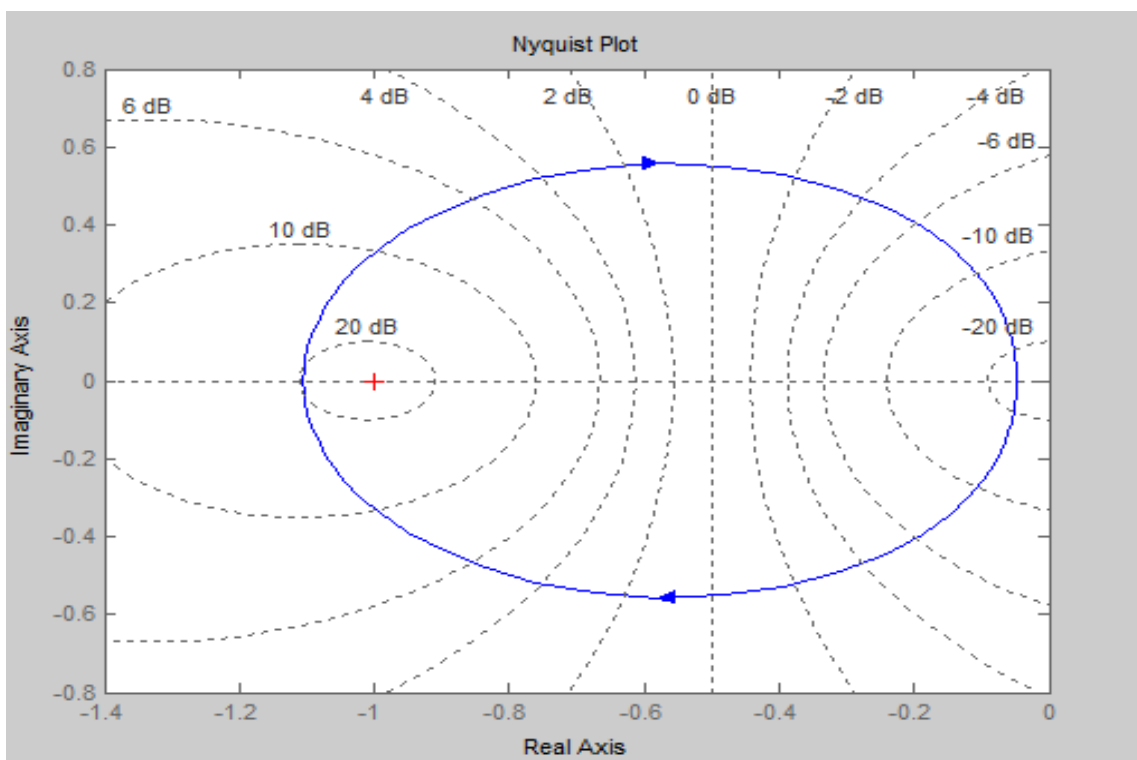


FIGURE 4.13: Nyquist Plot for the System.

4.7 Gear Ratio Gain

The gear ratio gain, G_r , is the ratio of the magnitude of the steady-state step response to the magnitude of the step input.

Results from Figure 4.14 showed that with a unit step input to the system, the output voltage varied with the gear ratio used. when the gear ratio is less than

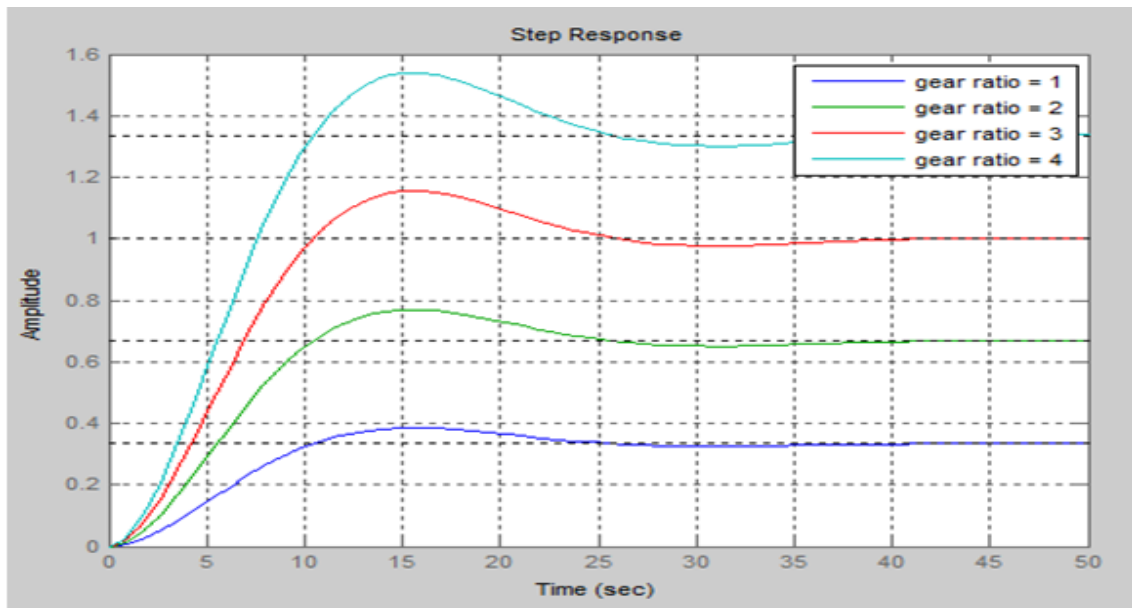


FIGURE 4.14: Step Response of the System for Different Values of Gear Ratio.

3, the output voltage of the system is less than the input voltage. When the gear ratio is equal to 3, the output voltage is equal to the input voltage and when the gear ratio is more than 3, the output voltage is greater than the input voltage. This shows that to ensure excess voltage, the gear ratio should be greater than 3.

4.8 Bode Diagram

The Bode response plot was necessary to examine the stability of the loop. Gear ratio G_r is a proportional value that shows the relationship between the magnitudes of the input to the magnitude of the output signal at the steady state.

Many systems harbor a method by which the gear ratio can be altered, providing more or less power to the system. However, increasing gear ratio or decreasing gear ratio beyond a particular safety zone can cause the system to become unstable. As the gear ratio to a system increases, generally the rise-time decreases, the percent overshoot increases, and the settling time increases. Bode plots were determined graphically using Matlab software. The MATLAB script for observing

the bode plots for specified values of G_r shown in the appendix A. The simulation results indicated that;

- (i) $G_r = 1$, the system is stable and with slow response.
- (ii) $G_r = 3$, the system is stable and with good step response.
- (iii) $G_r = 8$, the system is stable and with quick response. The description is summarized in the Tables 4.4.

TABLE 4.4: *Phase Margin and Gain Margin of the Different Values of the Gear Ratio*

G_r	PM(deg)	Steady State	Overshoot	Peak Value	ST(s)	RT(s)
1	Inf	0.385	15.5	0.385	3.7	7.08
2	Inf.	0.769	15.5	0.769	3.7	7.08
3	92.5	1.000	15.5	1.150	3.7	7.08
4	68.8	1.330	15.5	1.540	3.7	7.08
5	57.5	1.670	15.5	1.920	3.7	7.08
6	50.4	2.000	15.5	2.310	3.7	7.08
7	45.3	2.330	15.5	2.690	3.7	7.08
8	41.5	2.670	15.5	3.080	3.7	7.08

From Table 4.4, it was observed that the gain margin is increasing with an increase in the gear ratio. Using stability criterion (Shirsavar, 2011), in order to have a nice power supply the phase margin should be greater 45^0 and the gain margin should be greater than 10dB, therefore the power supply is very good for the range $1 \leq G_r \leq 6$. This indicates a phase margin of above 45^0 . The corresponding closed-loop step response exhibits 15.5 % overshoot and some oscillations. From the Nyquist plot shown in Figure 4.15, it shows that the range of gear ratio is stable. Substituting values obtained from Simulink into equations (3.7) and (3.21); the following values were obtained in the Tables 4.5 and 4.6.

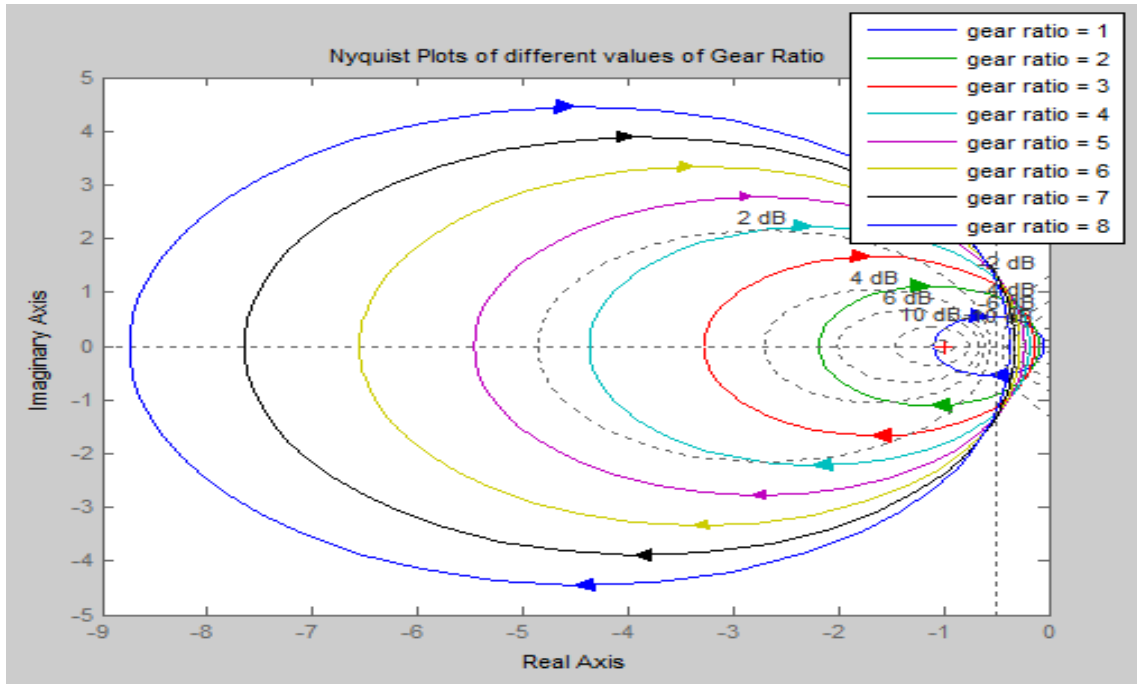


FIGURE 4.15: Nyquist Plot for Specified Values of Gear Ratio.

TABLE 4.5: *Motor Specification*

G_r	V	B	J	K	L	I	R	T	ω
1	12	1.60	7.16	0.41	5.74	0.28	1.71	2.7	22.03
2	12	1.60	7.16	0.41	5.74	0.28	1.71	2.7	22.03
3	12	1.60	7.16	0.41	5.74	0.28	1.71	2.7	22.03
4	12	1.60	7.16	0.41	5.74	0.28	1.71	2.7	22.03
5	12	1.60	7.16	0.41	5.74	0.28	1.71	2.7	22.03
6	12	1.60	7.16	0.41	5.74	0.28	1.71	2.7	22.03
7	12	1.60	7.16	0.41	5.74	0.28	1.71	2.7	22.03
8	12	1.60	7.16	0.41	5.74	0.28	1.71	2.7	22.03

It can be observed from Graphs shown in Figures 4.16 and 4.17 that the excess voltage and alternator frequency increase with an increase in Gear ratio. Therefore there is excess energy for $G_r > 3$.

TABLE 4.6: *Alternator Specification*

Gr	B	J	K	L	R	ω	v	excess Voltage
1	0.84	9.40	0.41	8.16	0.41	22.03	9.03	-2.97
2	0.84	9.40	0.41	8.16	0.41	44.06	18.06	6.06
3	0.84	9.40	0.41	8.16	0.41	66.09	27.10	15.1
4	0.84	9.40	0.41	8.16	0.41	88.12	36.13	24.13
5	0.84	9.40	0.41	8.16	0.41	110.15	45.16	33.16
6	0.84	9.40	0.41	8.16	0.41	132.18	54.19	42.19
7	0.84	9.40	0.41	8.16	0.41	154.21	63.23	51.23

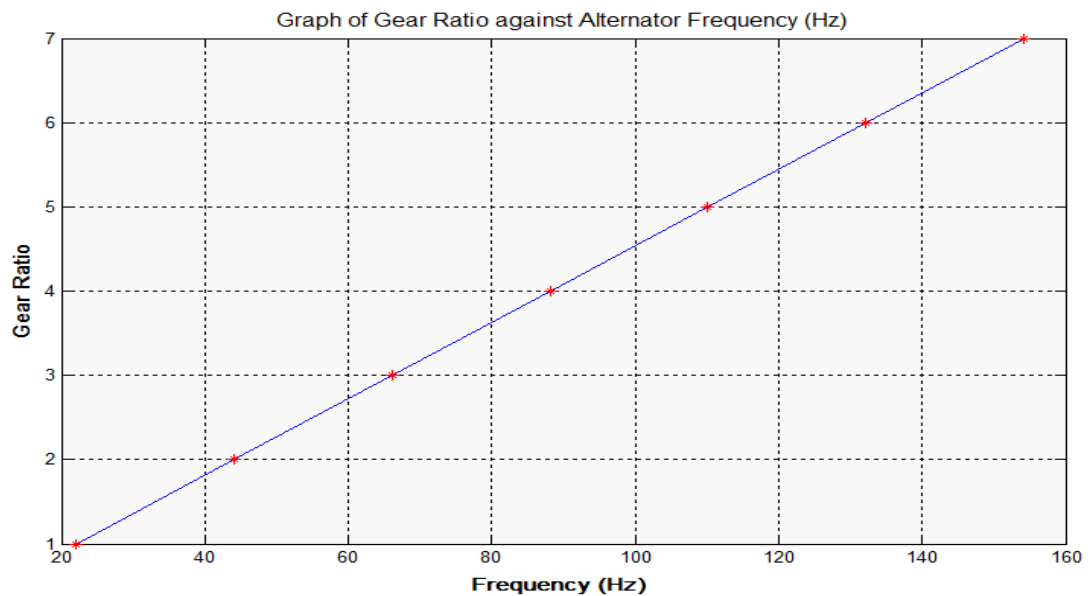


FIGURE 4.16: Graph of Gear Ratio against Alternator frequency.

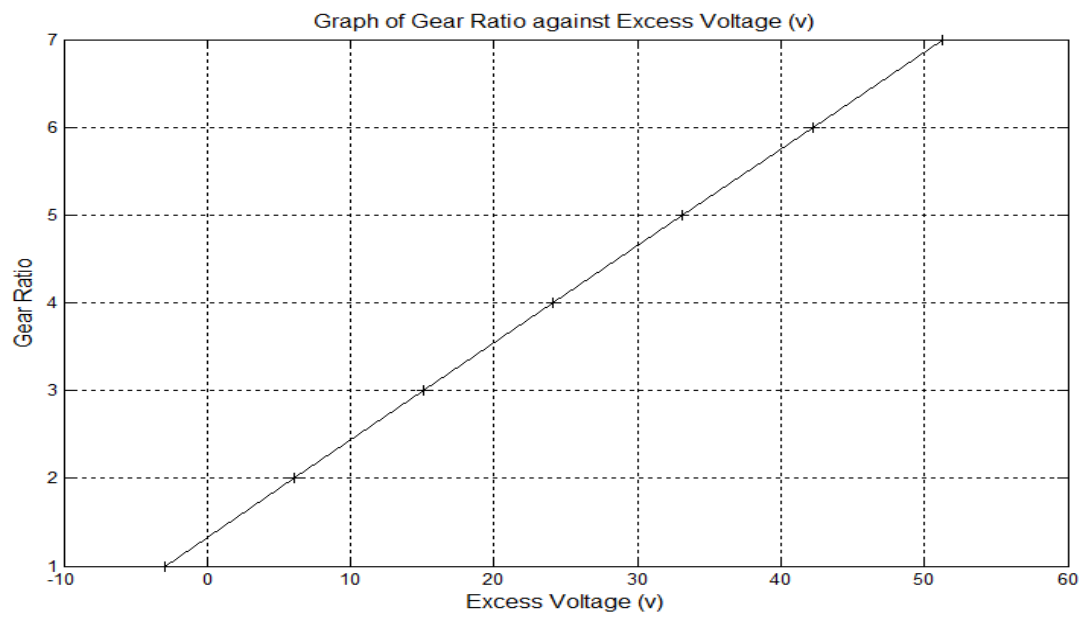


FIGURE 4.17: Graph of Excess Voltage (v) against Gear Ratio.

Chapter 5

Conclusion, Contributions and Recommendations

5.1 Conclusion

In this study, a mathematical model to represent the MGA dynamics was designed. Detailed mathematical derivations from first principles have been presented and then represented the derived equations within Simulink. The results showed that there is excess clean energy which can be utilized elsewhere for industrial and domestic use. The parameters identification was investigated by applying different methods in MGA models. The model parameters were estimated based on experimental measurements from National Electrical Construction and Maintenance data and through the use of nonlinear optimization numerical tools. It was shown that the chosen model is able to reproduce observed expected dynamics. The non-linear least-square and pattern-search strategies were the best methods among the methods studied because of their performance and the accuracy. Finally, the stability of the MGA Model was studied using Routh-Hurwitzs, Nyquist

and Bode plots. It was found that the Bode plot is the best tool for determining the range of the gear ratio and the Nyquist plot is best to obtain the relative stability of the closed system. Routh Hurwitz method is not the best because it does not give exact locations of stability points and does not suggest methods for stabilizing an unstable system though Stability can be judged without solving the characteristic equation of the open system.

5.2 Contributions

This research has contributed to the field of system modeling, system identification, and system stability analysis. This is a relatively new area that has a growing importance in control problems. The precise mathematical models are essential during the controller designing process. It is because they allow the designer to estimate the closed-loop behavior of the plant. The errors in parameter values could result in poor instability and control. Therefore, adequacy and accuracy of parameters identification are primary modeling problems that always had to be addressed. These contributions extend the understanding of the MGA response in assisting in control fields and designing robust controllers. The desire to have a clean energy source and clean environment prompted the investigator into this research. Also the need to cope with increasing electricity demand and to deal with problems emerging from unexpected blackouts motivated the author. Generating electricity from such renewable energy rather than fossil fuels offers significant public health benefits and curbs issues of a power outage.

5.3 Recommendation and Future Work

This study used a data acquisition module from national instruments to get the required experimental signals. Interfacing and identification process is built and done using the MATLAB or Simulink in PC. Good future work may be if the researcher can apply the acquiring and the identification process using microcontrollers or embedded controllers such as Field Programmable Gate Array (FPGA) or Digital Signal Processor (DSP) controllers, this will serve the cost of DAQ and PC used in this work. A design intended to produce a portable and small size system will be desirable. Finally, the study strongly recommends energy policies and technologies that could phase-out coal, limit barriers to the growth and progressive exploitation of renewable energy, and design a cost-effective, and sustainable clean energy economy.

References

- Ahmed, S., Huang, B., & Shah, S. L. (2007). Novel identification method from step response. *Control Engineering Practice*, 15(5), 545–556.
- Aleksashkin, A., Mikkola, A., et al. (2008). *Literature review on permanent magnet generators design and dynamic behavior*. Lappeenranta University of Technology.
- Alshikh, A. A. (2016). Solving ordinary differential equations with variable coefficients. *Journal of Progressive Research in Mathematics*, 10(1), 1454–1459.
- Antonanzas, J., Osorio, N., Escobar, R., Urraca, R., Pison, F. Martinez-de, & Antonanzas-Torres, F. (2016). Review of photovoltaic power forecasting. *Solar Energy*, 136, 78–111.
- Ayres, R. U., Bergh, J. C. Van den, Lindenberger, D., & Warr, B. (2013). The underestimated contribution of energy to economic growth. *Structural Change and Economic Dynamics*, 27, 79–88.
- Balabanian, N., & Lepage, W. R. (1956). What is a minimum-phase network? *Transactions of the American Institute of Electrical Engineers, Part I: Communication and Electronics*, 74(6), 785–788.
- Barmish, B. (1984). Invariance of the strict hurwitz property for polynomials with perturbed coefficients. *IEEE transactions on automatic control*, 29(10), 935–936.
- Basilio, & Moreira, M. V. (2004). State-space parameter identification in a second control laboratory. *IEEE Transactions on Education*, 47(2), 204–210.
- Basilio, J., & Matos, S. (2002). Design of pi and pid controllers with transient performance specification. *IEEE Transactions on Education*, 45(4), 364–370.
- Beaty, H. W., & Kirtley, J. L. (1998). *Electric motor handbook*. McGraw-Hill Professional.
- Bejan, A. (2016). *Advanced engineering thermodynamics*. John Wiley & Sons.
- Belgacem, F. B. M., & Silambarasan, R. (2013). Laplace transform analytical restructure. *Applied Mathematics*, 4(06), 919.
- Bell, R., & Åström, K. J. (1987). *Dynamic models for boiler-turbine-alternator*

units: data logs and parameter estimation for a 160 mw unit. Lund Institute of Technology, Department of Automatic Control.

- Bode, H. W., et al. (1945). Network analysis and feedback amplifier design.
- Box, G. E., Jenkins, G. M., Reinsel, G. C., & Ljung, G. M. (2015). *Time series analysis: forecasting and control*. John Wiley & Sons.
- Cluett, W., & Wang, L. (1991). Modelling and robust controller design using step response data. *Chemical engineering science*, 46(8), 2065–2077.
- Dhunde, R. R., & Waghmare, G. (2016). Double laplace transform combined with iterative method for solving non-linear telegraph equation. *Journal of the Indian Mathematical Society*, 83(3-4), 221–230.
- Dorf, R. C., & Bishop, R. H. (2011). *Modern control systems*. Prentice Hall.
- Fliess, M., & Sira-Ramirez, H. (2008). Closed-loop parametric identification for continuous-time linear systems via new algebraic techniques. In *Identification of continuous-time models from sampled data* (pp. 363–391). Springer.
- Gardner, M. (1942). *J.: L. barnes, transients in linear systems, vol. 1*. Wiley New York.
- Goldstein, J., & Soltan, M. (2000). Dc, linear ac and nonlinear ac stability analysis using bifurcation and nyquist theory. *Microwave Journal*, 43(5), 278.
- Golnaraghi, F., & Kuo, B. C. (2010). Automatic control systems. *Complex Variables*, 2, 1–1.
- Grover, M., Kumar, B. L., & Ramalla, I. (2014). The free energy generator.
- Hopgood, A. A. (2011). *Intelligent systems for engineers and scientists*. CRC press.
- Hurwitz, A. (1964). On the conditions under which an equation has only roots with negative real parts. *Selected papers on mathematical trends in control theory*, 65, 273–284.
- James, H. M., Nicholas, N. B., & Phillips, R. S. (1947). *Theory of servomechanisms* (Vol. 25). McGraw-Hill Book Co.
- Jose, V., et al. (2016). Modelling of greenhouse gas emission from livestock. *Front. Environ. Sci*, 85(10), 1-10.
- Kish, L. B. (2006). Totally secure classical communication utilizing johnson (-like) noise and kirchoff's law. *Physics Letters A*, 352(3), 178–182.
- Koech, W., Rotich, S., Rotich, T., & Nyamwala, F. (2016). Dynamic model of a dc motor-gear-alternator (mga) system. *Asian Research Journal of Mathematics*, 1, 1-16.
- Kumar, D., Singh, J., & Rathore, S. (2012). Sumudu decomposition method

- for nonlinear equations. In *International mathematical forum* (Vol. 7, pp. 515–521).
- Liu, Y., Xie, L., & Ding, F. (2009). An auxiliary model based on a recursive least-squares parameter estimation algorithm for non-uniformly sampled multirate systems. *Proceedings of the Institution of Mechanical Engineers, Part I: Journal of Systems and Control Engineering*, 223(4), 445–454.
- Mamani, G., Becedas, J., Feliu-Batlle, V., & Sira-Ramirez, H. (2007). Open-loop algebraic identification method for a dc motor. In *Control conference (ecc), 2007 european* (pp. 3430–3436).
- Mamani, G., Becedas, J., Feliu-Batlle, V., & Sira-Ramírez, H. (2008). Algebraic observers to estimate unmeasured state variables of dc motors. *Engineering Letters*, 16(2).
- Mandal, A. K. (2006). *Introduction to control engineering: Modeling, analysis and design*. New Age International.
- Marquardt, D. W. (1963). An algorithm for least-squares estimation of nonlinear parameters. *Journal of the society for Industrial and Applied Mathematics*, 11(2), 431–441.
- Martin, N. J., & Rice, J. L. (2012). Developing renewable energy supply in queensland, australia: A study of the barriers, targets, policies and actions. *Renewable Energy*, 44, 119–127.
- McFadden, D. (1989). A method of simulated moments for estimation of discrete response models without numerical integration. *Econometrica: Journal of the Econometric Society*, 995–1026.
- Moner, M., Ghanadan, R., Solano-Peralta, M., Kougiyas, I., Bódis, K., Huld, T., et al. (2016). Adaptation of feed-in tariff for remote mini-grids: Tanzania as an illustrative case. *Renewable and Sustainable Energy Reviews*, 53, 306–318.
- Moner-Girona, M., Bódis, K., Huld, T., Kougiyas, I., & Szabó, S. (2016). Universal access to electricity in burkina faso: scaling-up renewable energy technologies. *Environmental Research Letters*, 11(8), 084010.
- Mottershead, J., & Friswell, M. (1993). Model updating in structural dynamics: a survey. *Journal of sound and vibration*, 167(2), 347–375.
- Nelles, O. (2013). *Nonlinear system identification: from classical approaches to neural networks and fuzzy models*. Springer Science & Business Media.
- Niu, X. (2013). *Modeling and design analysis of a permanent magnet linear synchronous generator* (Tech. Rep.). Tech. rep. UIUC-ESDL-2013-01. Engineering System Design Lab.
- Nyquist, H. (1932). Regeneration theory. *Bell system technical journal*, 11(1), 126–147.

- Olsthoorn, D., Haghghat, F., & Mirzaei, P. A. (2016). Integration of storage and renewable energy into district heating systems: A review of modelling and optimization. *Solar Energy*, *136*, 49–64.
- Orbach, Y., & Fruchter, G. E. (2011). Forecasting sales and product evolution: The case of the hybrid/electric car. *Technological Forecasting and Social Change*, *78*(7), 1210–1226.
- Pan, Y., Birdsey, R. A., Fang, J., Houghton, R., Kauppi, P. E., Kurz, W. A., et al. (2011). A large and persistent carbon sink in the worlds forests. *Science*, *333*(6045), 988–993.
- Pérez-Lombard, L., Ortiz, J., & Pout, C. (2008). A review on buildings energy consumption information. *Energy and buildings*, *40*(3), 394–398.
- Rabbani, M. J., Hussain, K., Ali, A., et al. (2013). Model identification and validation for a heating system using matlab system identification toolbox. In *Iop conference series: Materials science and engineering* (Vol. 51, p. 012022).
- Razykov, T. M., Ferekides, C. S., Morel, D., Stefanakos, E., Ullal, H. S., & Upadhyaya, H. M. (2011). Solar photovoltaic electricity: Current status and future prospects. *Solar Energy*, *85*(8), 1580–1608.
- Rice, M., & Cutler, S. K. (2012). *Clinical research in occupational therapy*. Cengage Learning.
- Rizk, J., & Nagrial, M. (2000). Design of permanent-magnet generators for wind turbines. In *Power electronics and motion control conference, 2000. proceedings. ipemc 2000. the third international* (Vol. 1, pp. 208–212).
- Roca, L., & Duguleană, M. (2016). An online observer for minimization of pulsating torque in smpm motors. *PloS one*, *11*(4), e0153255.
- Saavedra-Montes, A. J., Ramos-Paja, C. A., & Ramírez, J. M. (2012). A systematic review on identification of excitation systems for synchronous generators. *Revista EIA*(18), 33–48.
- Salah, M. S. (2015). *Parameters identification of a permanent magnet dc motor*. Unpublished doctoral dissertation, The Islamic University of Gaza.
- Shirsavar, D. A. (2011). Designing stable digital power supplies. *Biricha Digital Power Ltd*.
- Shumway-Cook, A., & Woollacott, M. H. (2010). *Motor control: theory and practical applications*. Williams & Wilkins.
- Silverman, L. M., & Anderson, B. D. (2012). Controllability, observability and stability of linear systems. *SIAM Journal on control*, *6*(1), 121–130.
- Sinha, N. K. (2008). *Control systems*. New Age International.
- Špoljarić, Ž., Miklošević, K., & Jerković, V. (2010). Synchronous generator modeling using matlab. In *Sip 2010 28th international conference science in*

practice.

- Stépán, G., & Insperger, T. (2006). Stability of time-periodic and delayed systems a route to act-and-wait control. *Annual Reviews in control*, 30(2), 159–168.
- Sudhakar, T., Rajan, M. R., Srinivasan, K., Prabu, R. R., Narmadha, T., & Krishnan, M. M. (2016). Modeling and simulation of distribution network with the integration of distribution generator using matlab. *Indian Journal of Science and Technology*, 9(12).
- Tarantola, A. (2005). *Inverse problem theory and methods for model parameter estimation*. SIAM.
- Tükenmez, M., & Demireli, E. (2012). Renewable energy policy in turkey with the new legal regulations. *Renewable Energy*, 39(1), 1–9.
- Urone, P., & Hinrichs, R. (2016). *College physics*.
- Vas, P. (1998). *Sensorless vector and direct torque control*. Oxford University Press, USA.
- Wójcik, M., Szukiewicz, M., & Kowalik, P. (2014). The application of the laplace transform for modeling of gas flow using maple. *Journal of Applied Computer Science Methods*, 6(1), 43–53.
- Wu, Z., Dai, W., Man, M., & Luo, E. (2012). A solar-powered traveling-wave thermoacoustic electricity generator. *Solar Energy*, 86(9), 2376–2382.
- Yusuf, S., Samosir, A., & Abdulkadir, M. (2012). Simplified model of a dc rotating machine for mechanical energy generation using matlab/simulink. *International Journal of Engeneering and Innovative Technology (IJEIT)*, 2(6).
- Zhang, Q., & Messner, W. C. (2011). Root locus design with complex proportional-integral-lead compensation. In *Proceedings of the 2011 american control conference* (pp. 693–698).

Appendices

A. MATLAB Scripts Used for Simulating the MGA Model

A.1 Parameter Estimation

```
%%%%%%%%%%%%%%%%%%%%%%%%%%%%%%%%%%%%%%%%%%%%%%%%%%%%%%%%%%%%%%%%%%%%%%%%%
```

```
File: parameters.m
```

```
% Author: Cheruiyot w. Koech
```

```
% email: koech80@gmail.com
```

```
% Department of Mathematics and Physics
```

```
% Moi University
```

```
% June, 2017
```

```
%%%%%%%%%%%%%%%%%%%%%%%%%%%%%%%%%%%%%%%%%%%%%%%%%%%%%%%%%%%%%%%%%%%%%%%%%
```

```
% MATLAB script for parameter estimation
```

```
function createline(XData1, YData1, Parent1)
```

```
%CREATELINE(XDATA1,YDATA1,PARENT1)
```

```
% XDATA1: line xdata
```

```
% YDATA1: line ydata
```

```
% PARENT1: line parent
```

```
% Auto-generated by MATLAB on 01-Jun-2017 12:00:46
```

```
% Create line
```

```
line(XData1,YData1,'Parent',Parent1,'LineWidth',1,'Color',[0 0 1]);
```

A.2 Step Response

```
%%%%%%%%%%%%%%%%%%%%%%%%%%%%%%%%%%%%%%%%%%%%%%%%%%%%%%%%%%%%%%%%%%%%%%%%%
```

```
File: Step Response.m
```

```
% Author: Cheruiyot w. Koech
```

```
% email: koech80@gmail.com
```

```
% Department of Mathematics and Physics
```

```
% Moi University
```

```
% June, 2017
```

```
%%%%%%%%%%%%%%%%%%%%%%%%%%%%%%%%%%%%%%%%%%%%%%%%%%%%%%%%%%%%%%%%%%%%%%%%%
```

```
% MATLAB script for step response
```

```
>> sys = tf([-58.59 -9.8 -0.14],[53.93 25.23 2.94])
```

```
g=[1,2,3,4,5,6,7,8]%Gr=1,2 etc
```

```
step(sys)
```

```
S = stepinfo(sys,'RiseTimeLimits',[0.05,0.95])
```

```
legend('gear ratio = 1','gear ratio = 2','gear ratio = 3',
```

```
'gear ratio = 4', 'gear title ('step response')
```

```
grid on
```

```
Transfer function:
```

$$-58.59 s^2 - 9.8 s - 0.14$$

$$53.93 s^2 + 25.23 s + 2.94$$

A.3 Bode plot

%%%

File: Bode plot.m

% Author: Cheruiyot w. Koech

% email: koech80@gmail.com

% Department of Mathematics and Physics

% Moi University

% June, 2017

%%%

% MATLAB script for Bode Plot

```
>> sys = tf([-58.59 -9.8 -0.14],[53.93 25.23 2.94])
```

```
g=[1,2,3,4,5,6,7,8]%Gr=1,2 etc
```

```
step(sys)
```

```
S = stepinfo(sys,'RiseTimeLimits',[0.05,0.95])
```

```
legend('gear ratio = 1','gear ratio = 2','gear ratio = 3',
```

```
'gear ratio = 4', 'gear bode(sys);
```

```
Title Bode Plots of different values of Gear Ratio
```

```
Transfer function:
```

$$-58.59 s^2 - 9.8 s - 0.14$$

 53.93 s² + 25.23 s + 2.94

A.4 Nyquist

%%%

File: Nyquist.m

% Author: Cheruiyot w. Koech

% email: koech80@gmail.com

% Department of Mathematics and Physics

% Moi University

% June, 2017

%%%

The Nyquist plot is drawn by using the MATLAB function Nyquist

```
>> sys = tf([-58.59 -9.8 -0.14],[53.93 25.23 2.94])
```

```
g=[1,2,3,4,5,6,7,8]%Gr=1,2 etc
```

```
step(sys)
```

```
S = stepinfo(sys,'RiseTimeLimits',[0.05,0.95])
```

```
legend('gear ratio = 1','gear ratio = 2','gear ratio = 3',
```

```
'gear ratio = 4','gear nyquist(sys);
```

Title Nyquist Plots of different values of Gear Ratio

Transfer function:

-58.59 s² - 9.8 s - 0.14

$$53.93 s^2 + 25.23 s + 2.94$$

A.5 Gain and Phase Margins

%%%

File: Gain and Phase Margins.m

% Author: Cheruiyot w. Koech

% email: koech80@gmail.com

% Department of Mathematics and Physics

% Moi University

% June, 2017

%%%

The gain and phase margins by using the MATLAB function

```
>> sys = tf([-58.59 -9.8 -0.14],[53.93 25.23 2.94])
```

```
g=[1,2,3,4,5,6,7,8]%Gr=1,2 etc
```

```
legend('gear ratio = 1','gear ratio = 2','gear ratio = 3',
```

```
'gear ratio = 4', 'gear [Gm, Pm, wg, wp] = margin (sys);
```

% The last line of the command provides GM, PM along with the

phase crossover frequency wg (associated with GM) as well as gain

crossover frequency wp (associated with PM) of the loop gain sys.

Transfer function:

$$-58.59 s^2 - 9.8 s - 0.14$$

$$53.93 s^2 + 25.23 s + 2.94$$

```
function createaxes(Parent1, XData1, YData1, XData2, YData2)
%CREATEAXES(PARENT1,XDATA1,YDATA1,XDATA2,YDATA2)
% PARENT1: axes parent
% XDATA1: line xdata
% YDATA1: line ydata
% XDATA2: line xdata
% YDATA2: line ydata
% Auto-generated by MATLAB on 01-Jun-2017 18:15:27
% Create axes
axes1 = axes('Parent',Parent1,...
'YTickLabel',{'0','','','','0.75','','','1.5'},...
'YGrid','on',...
'YColor',[0.4 0.4 0.4],...
'XGrid','on',...
'XColor',[0.4 0.4 0.4],...
'Position',[0.1441 0.11 0.7609 0.7788],...
'FontSize',8);
% Uncomment the following line to preserve the X-limits of the axes
% xlim(axes1,[0 50]);
% Uncomment the following line to preserve the Y-limits of the axes
% ylim(axes1,[0 0.4]);
% Uncomment the following line to preserve the Z-limits of the axes
% zlim(axes1,[-10 13]);
box(axes1,'on');
```

```
% Create line
line(XData1,YData1,'Parent',axes1,'Visible','off','Color',[0 0 1]);

% Create hgroup
hgroup1 = hgroup('Parent',axes1,'DisplayName','sys');

% Create line
line(XData2,YData2,'Parent',hgroup1,'LineWidth',2,'Color',[0 0 1]);
```

B. List of Publications

- B.1** Koech, W.C., Rotich, S., Rotich, T., and Nyamwala, F.O. (2016) Dynamic Model of a DC Motor-gear-alternator (MGA) System. *Asian Research Journal of Mathematics*, 1(4), 1-16.
- B.2** Koech, W.C., Rotich, T., Nyamwala, F.O. and Rotich, S. (2016) Parameter Estimation of a DC Motor-Gear-Alternator (MGA) System via Step Response Methodology. *American Journal of Applied Mathematics*, 4(5), 252-257.